NSEC-7

RADIOACTIVE WASTE

RETENTION EFFICIENCIES OF CHARCOAL TRAPS FOR FISSION GASES

Technical Report

By
R. C. Koch
G. L. Grandy

August 23, 1957

Nuclear Science and Engineering Corporation
Pittsburgh, Pennsylvania

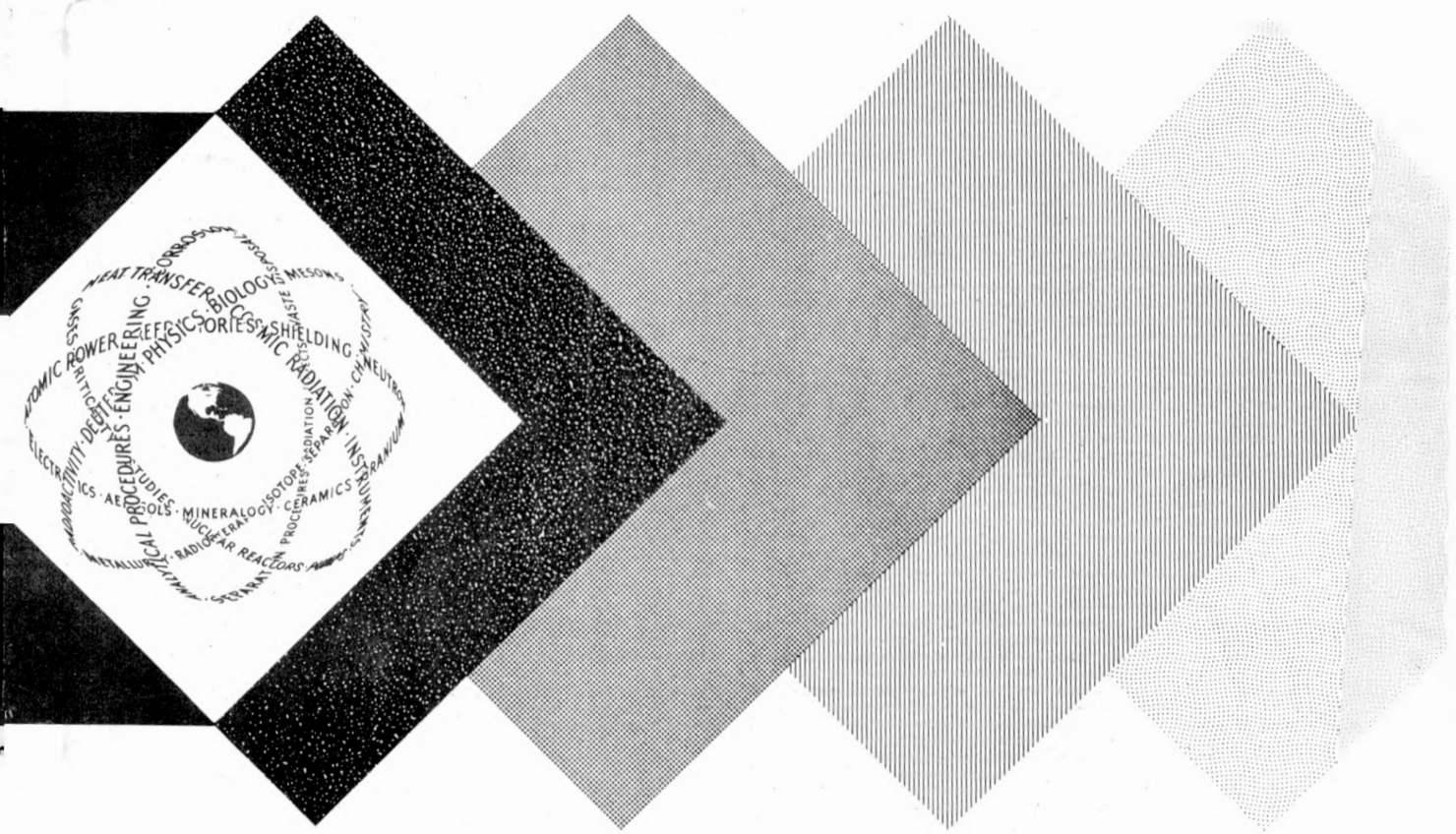

UNITED STATES ATOMIC ENERGY COMMISSION
Technical Information Service

LEGAL NOTICE

Printed in USA. Price $1.75. Available from the Office of Technical Services, Department of Commerce, Washington 25, D. C.

AEC Technical Information Service Extension
Oak Ridge, Tennessee

NSEC-7

TECHNICAL REPORT

RETENTION EFFICIENCIES OF CHARCOAL TRAPS FOR FISSION GASES

R. C. Koch and G. L. Grandy

Chemistry Department

August 23, 1957

NUCLEAR SCIENCE AND ENGINEERING CORPORATION
P. O. Box 10901 Pittsburgh 36, Pa.

I. Introduction

An investigation has been undertaken to determine the efficiency of certain charcoal traps for tracer quantities of fission product gases in the presence of macro quantities of a nonisotopic purge, or carrier, gas. The investigation included observation of the effects of charcoal particle size, trap temperature, and carrier gas flow rate on the retention times of the tracer gases in the traps. The main emphasis of these studies was to determine the behavior of xenon and krypton under the experimental conditions, but a limited number of experiments were performed using radioactive iodine as the tracer.

Browning and Bolta[1] have reported the results of a series of similar measurements on -8+14 mesh Columbia ACA charcoal using radiokrypton as the tracer and nitrogen as the carrier gas. Their results indicated that the efficiency of their traps, at a constant carrier gas flow rate, was a function of trap temperature, trap dimensions and the composition of the carrier gas. These workers measured the retention efficiency in terms of three parameters: (1) the time delay from injection of the charge of tracer gas into the carrier flow upstream of the trap to its appearance downstream of the trap, (2) the elapsed time until the maximum elution rate of the tracer was observed, and (3) the elapsed time until the total quantity of tracer was eluted. Browning and Bolta also observed that, for a given trap, flow rate and carrier gas, these delay times decreased with increasing temperature. In general, a decrease in delay time was accompanied by a corresponding increase in the maximum elution rate of the tracer. Furthermore, at constant temperature and flow rate, doubling the trap length was observed to double the delay time for maximum elution rate. Substitution of helium

for nitrogen as the carrier gas substantially increased the trap efficiency since helium is only slightly adsorbed by charcoal under the experimental conditions.

Browning and Bolta successfully correlated their experimental results using an expression derived from theoretical considerations analogous to the continuous dilution tank problem. They assumed that a series of N charcoal-filled chambers comprises each trap, each chamber being defined as that volume in which the tracer is instantaneously brought to adsorption equilibrium as it enters. Browning and Bolta showed the general expression for P_N, the equilibrium pressure of tracer in the Nth chamber, to be

$$P_N = \frac{AN^N(Ft)^{(N-1)}e^{-NFt/(km)}}{(N-1)\,!\,(km)^N} \qquad (1)$$

where A = the total amount of tracer injected into the first chamber, (cm^3 atm)

N = the number of theoretical chambers

F = the volume rate of flow of the carrier gas, ($cm^3\ sec^{-1}$)

t = the elapsed time after injection of the tracer, (sec)

m = the mass of charcoal in the trap, (grams)

k = a constant derived from the slope of the isotherm for adsorption of the tracer in a mixture of the tracer and carrier gases, ($cm^3\ gram^{-1}$)

(km)= a measure of the adsorptive capacity of the trap for the tracer under the conditions of the measurement.

Browning and Bolta give the following expressions for t_{max} and P_{max}, the elapsed time and tracer pressure when the elution rate is at a maximum:

$$t_{max} = \frac{(N-1)(km)}{NF} \qquad (2)$$

$$P_{max} = \frac{AN(N-1)^{(N-1)}e^{-(N-1)}}{(N-1)\,!\,(km)} \qquad (3)$$

Using these three equations, Browning and Bolta calculated values of (km) and N for each

experiment. They found that N for a given trap and carrier gas was independent of temperature, and that the logarithm of the quantity (km) was inversely proportional to the absolute temperature of the trap.

The present program was designed to extend this technique to several flow rates, temperatures, and charcoal particle sizes using nitrogen as the carrier gas. The experimental data for krypton were to be compared with those of Browning and Bolta in an attempt to correlate the data and to test the applicability of the theoretical treatment at the conditions under which these experiments were performed.

II Apparatus

The apparatus used in these investigations is shown schematically in Figure 1. The essential portions of the flow system include a source of compressed nitrogen, a purification system, a flow-rate meter, an injection manifold, two identical charcoal traps in parallel, a monitor for detecting the radioactive tracer, a Cartesian manostat pressure regulator and a vacuum pump. The connecting lines are constructed of 0.5 in copper tubing. The purification system consists of a bed of charcoal in series with a drying tube to remove any particulate matter, moisture, or other adsorbable gases from the nitrogen stream. The injection manifold was a 3-ft length of copper tubing isolated by two toggle valves. A bypass permits the isolation of the injection manifold without interruption of the carrier flow. Toggle valves are provided to permit rapid change of flow between the two manifolds. The traps are stainless steel U-tubes having an inside diameter of about 0.40 in. They contain a 16-in long adsorbent bed holding about 25 grams of charcoal. Activated cocoanut charcoal obtained from Fisher Scientific Company was used. The traps are connected to the system with swage-lock fittings. The trap temperature is measured with a stainless steel clad, copper-constantan

thermocouple inserted into the trap through a special swage-lock fitting at the downstream end. The cladding is welded at the junction. The thermocouple extends almost to the bottom of the trap.

Downstream from the traps, the system consists of 0.5-in copper tubing which passes through the monitor shield and past the detector. For the xenon experiments, a 1.5-in by 1-in NaI crystal in conjunction with a photomultiplier tube served as the detector. The crystal was placed adjacent to the copper tubing and monitored the gamma radiation from the tracer as it passed after elution from the traps. For the krypton and iodine work, the crystal was replaced by an end-window Geiger tube which monitored the beta radiation from the passing tracer. For these tests, a short length of polyethylene tubing replaced in the copper line at the detector to minimize activity losses due to absorption of the beta particles in the copper tubing.

The output from either detector was registered by a scaler with a two microsecond resolution time. The scaler drives an Ametron recorder which prints the cumulative scaler output during equal time intervals. For most of this work, the Ametron interval was 18 seconds, the shortest period at which the instrument will operate.

In addition to the main flow system, an auxiliary system for preparing tracer charges is provided. This system consists of a short, 3/8-in copper manifold provided with a bomb containing the tracer, a pressure gauge, and facilities for evacuation and for introducing carrier gas. This system connects directly to the main flow system through the injection manifold.

III. Experimental Techniques

A typical sequence of operations for a single test proceeded in the following manner. The tracer, mixed with nitrogen at a pressure of several atmospheres, was contained in the bomb attached to the charge preparation system. This system, along

with the injection manifold, was evacuated. A charge of tracer was bled into this system to a predetermined low pressure. A stream of nitrogen was passed into the system to sweep the tracer into the injection manifold. The valve between the two manifolds was closed when the system pressure was one atmosphere and before the nitrogen flow was stopped. In this manner, an efficiency of better than 90 percent was obtained for the transfer of the tracer to the injection manifold. Simultaneously, the trap was brought to temperature, and the desired nitrogen flow rate was established through the trap using the bypass manifold. The tracer was injected by opening the two toggle valves on the injection manifold and closing the bypass simultaneously. The injection was timed to correspond to a print-out of the Ametron recorder. The nitrogen continued to sweep through the system until the Ametron indicated that all the tracer had been eluted from the trap and until a monitor background check had been obtained.

The above procedure proved satisfactory for krypton and xenon, but several attempts to introduce radioactive iodine into the system in the same manner failed since the iodine condensed in the copper system before reaching the traps. Therefore, the apparatus was modified as illustrated in Figure 2. One of the charcoal traps was removed from the system, and a glass apparatus was installed to replace the metal system leading from the trap inlet to the monitor. The glass apparatus consists primarily of a trap of the same dimensions as the steel trap. A thin-diameter sidearm is provided on the upstream side of the trap for preparation and injection of the iodine tracer. A needle valve permits regulation of a small fraction of carrier flow through the sidearm. The tracer, in the form of a few drops of a solution of carrier-free NaI, was placed in the sidearm and evaporated to dryness. A small crystal of iodine was then placed in the sidearm, the system was closed, and the flow rate and trap temperature were established. A small fraction of the nitrogen flow was diverted through the sidearm. The sidearm was

then heated to induce exchange between tracer and carrier iodine and to sublime the iodine. The nitrogen swept the iodine gas to the charcoal trap. After a 10 to 15 second period of heating, the iodine was transferred quantitatively to the charcoal. At this time, the flow was stopped to permit monitoring of the trap. All the iodine was found to be retained within the first inch of charcoal. The flow was then re-established for the duration of the experiment.

IV Experimental Results

A. Krypton

The studies of the retention efficiencies for krypton were carried out using Kr^{85} as the tracer gas. Experiments were performed at four flow rates, 40 ft/min, 80 ft/min, 160 ft/min, and 300 ft/min, at each of three charcoal temperatures, -80°C, 0°C, and 100°C, in order to determine the effects of temperature and carrier gas flow rate on trap efficiency. The effect of charcoal particle size was studied using two traps containing -40+50 mesh charcoal and -20+30 mesh charcoal, respectively. Duplicate measurements were made on each trap at each temperature and flow rate.

The experimental data obtained from the Ametron recorder are the average counting rates of the eluted tracer as monitored by the detector during the successive recording periods, which were usually eighteen seconds. These data are readily described by histogram plots of the activity as a function of elapsed time after injection of the tracer. The elution patterns were normalized to an arbitrary value of the total activity so that the area under all of the histograms is the same. This normalization facilitated the preparation of composite curves from duplicate measurements and also the comparison of results obtained under different conditions.

The experimental elution curves obtained using -40+50 mesh charcoal as the adsorbent are shown in Figures 3 through 9. These histograms, as well as the others

which follow, are composites derived from duplicate determinations. Figures 3, 4 and 5 show the effect of flow rate on retention efficiency at 100°C, 0°C, and -80°C, respectively. Figures 6, 7, 8 and 9 represent the same data illustrating the effect of temperature on retention efficiency at constant flow rates of 40,80, 160 and 300 ft/min. The breakthrough points at 100°C and 0°C in these figures are drawn at the elapsed times required for normal flow at the several flow rates from the injection manifold through the system to the monitor. These times are 13.5, 6.8, 3.4 and 1.8 seconds, respectively, for flow rates of 40,80, 160 and 300 ft/min. It can be seen by inspection of Figures 3 through 5 that the times to breakthrough, maximum elution, and disappearance generally decrease with increasing flow. In Figures 6 through 9 a distinct increase in retention efficiency with decreasing temperature was observed. It should be noted that the times involved in these curves are very short, the peak times varying from a little less than a minute to only a few seconds.

The experimental data obtained using -20+30 mesh charcoal as the absorbent are shown in Figures 10 through 16. Figures 10, 11 and 12 illustrate the effects of flow rate on retention efficiency for trap temperatures of 100°C, 0°C, and -80°C, respectively. Again, the expected decrease in the times for breakthrough, peak and disappearance of the tracer was observed. Figures 13 through 16 show the same data plotted to illustrate the effect of temperature on retention efficiencies. The general observations on these data are the same as those deduced from data for the finer mesh charcoal. The larger mesh charcoal appears to provide a slightly greater efficiency in that the peak and disappearance times for a given set of conditions are generally somewhat longer.

In order to determine more accurately the values of the breakthrough times, peak times, and disappearance times for the elution curves, each histogram was

converted to a smooth curve. The curves were drawn so that they represented the same total activity as the histograms. The breakthrough time, peak time, and disappearance time for each curve was then obtained by inspection. Since the elapsed time involved for most of these curves were of the order of seconds or a few minutes, the time required for the gas flow through the system was frequently a significant portion of the elapsed time. Consequently, the characterizing times read from the curves were corrected for the flow times in the system. The corrected values for -40+50 mesh charcoal are shown in Table I and for -20+30 mesh charcoal are shown in Table II.

For -40+50 mesh charcoal, the peak times varied from 139 sec for the slowest flow rate at -80°C to about 7 sec for the fastest flow rate at 100°C. The corresponding disappearance times were 288 sec and 48 sec, while the range of breakthrough times was from 40 sec to zero. For -20+30 mesh charcoal the breakthrough times ranged from 36 sec to 0 sec, the peak times from 178 sec to 4 sec, and disappearance times from 871 sec to about 5 sec. The values in Tables I and II are estimated to be accurate to about ±4 sec, except for those which were obtained from runs of very short duration. These values probably have larger errors due to the difficulty of composing a curve from an insensitive histogram. In general, the data in the table confirm the trends deduced from the histograms. However, it can be seen that the peak time at a given temperature is not a linear function of the flow rate under the conditions of these tests, but that it varies more slowly than the flow rate. This behavior is not in agreement with that observed by Browning and Bolta[1]. The significance of these data will be discussed in a later section.

In addition to these experiments, a number of tests were performed using dry air as the carrier gas to search for a possible change in retention efficiency. Duplicate runs were made using each mesh charcoal at -80°C at flow rates of 40 ft/min and 80 ft/min.

The results are compared to those for nitrogen under the corresponding conditions in Figures 17 through 20. The histograms show approximately the same time dependence for both gases. The dispersion between the composite curves for nitrogen and oxygen is roughly the same as for the duplicate runs for each gas. These histograms were also converted to smooth curves to determine their characterizing times. The data are presented in Table III. Since no trend can be observed in comparing the data for the two gases, it may be concluded that a change of carrier gas from nitrogen to dry air will not materially affect the retention efficiency for the tracer.

B. Xenon

The studies of retention efficiencies for xenon were performed using the 5.27-day Xe^{133} as a tracer. The original scope of the xenon program was similar to the one for krypton, with an extension to a third charcoal particle size, -6+14 mesh. This phase of the program was interrupted when the limited supply of tracer was depleted, and it was discontinued when no more tracer was available. However, experiments were run at all four flow rates for the three charcoal particle sizes at 100°C and for selected conditions at other temperatures.

Data obtained using -40+50 mesh charcoal as the adsorbent at 100°C and 0°C are shown in Figures 22 and 23, respectively. These curves illustrate the effect of flow rate on retention efficiency. The same data, plotted to illustrate the temperature dependence of retention efficiency, are shown in Figures 24, 25 and 26. The variation of retention efficiency with temperature and flow rate for xenon is similar to that for krypton. However, the delay times appear substantially longer for xenon indicating that it is adsorbed more efficiently by the charcoal under these conditions.

The data obtained using -20+30 mesh charcoal at 100°C at the four flow rates are shown in Figure 27 and a determination at 0°C and 80 ft/min flow is shown in

Figure 28. The histograms derived from runs using -6+14 mesh at 100°C are presented in Figure 29, those at 0°C, in Figure 30, and that for a single determination at 80 ft/min flow at -80°C, in Figure 31. For each temperature, the histograms exhibit the same general dependence on flow rate and temperature as for krypton, except that the retention times for xenon are considerable greater.

The xenon histograms were treated in the same manner as those for krypton to determine more accurately the values of the breakthrough times, peak times, and disappearance times. The data for -40+50 mesh charcoal are presented in Table IV, those for -20+30 mesh, in Table V, and those for -6+14 mesh, in Table VI. The general trends observed in the xenon data are similar to those observed for krypton. The significance of these data will be discussed in a later section.

C. Iodine

A total of three iodine experiments were performed with 8.05-day I^{131} as tracer to estimate the efficiency of these traps for iodine. Using the special procedure described previously, iodine was introduced into a trap containing -20+30 mesh charcoal held at -80°C at a nitrogen flow rate of 40 ft/min. No iodine was observed at the monitor after 18.3 hr of operation. At this time, the test was terminated, and a survey of the trap showed no detectable movement of the tracer from the first inch of charcoal. A second test on an identical trap at -80°C with a flow rate of 300 ft/min continued for 5.1 hr with no detectable movement of the tracer. A final test was performed using -6+14 mesh charcoal held at 100°C at a flow rate of 300 ft/min. This test continued for 20.1 hr with no detectable movement of the tracer beyond the first inch

of charcoal. The results of these tests are shown in Table VII. It was observed that no motion of the adsorbed iodine occurred even at a trap temperature of 100°C when purged with a total volume of over 300 cubic feet of nitrogen. Upper limits of 15 percent and 0.5 in have been set for the fraction of the iodine which may have moved and the extent to which any appreciable motion may have occurred.

An auxiliary test was performed on one trap after it was removed from the system. The trap was heated to red heat for several minutes in an attempt to desorb the iodine. After cooling it was found that essentially all of the tracer was still present. The charcoal was then removed from the trap and the activity was found to be associated with the charcoal. In view of the apparent high efficiency of retention of the tracer, the decay of a small portion of it was counted to check the half-life and gamma spectrum. These measurements confirmed that the activity was due only to I^{131}. Therefore, it may be concluded that charcoal traps have a very high efficiency for retention of adsorbed iodine at temperatures as high as 100°C.

V. Comparison of Experiment with Theory

It has been mentioned in the Introduction that Browning and Bolta[1] have successfully correlated their data utilizing theoretical considerations based on a model analogous to the infinite dilution tank model. A modification of their method has been used to evaluate the present data and to compare the behavior of the tracer gases under the rather extreme flow conditions in these tests with those under nearly ideal conditions in the ORNL work. Under the modified method, we define P_i as

$$P_i = \frac{P_{max}}{i} \qquad (4)$$

It also follows from equation (3), p. 2, that

$$P_i = \frac{A\, N(N-1)^{(N-1)} e^{-(N-1)}}{i\,(N-1)!\,(km)} \qquad (5)$$

Equating the right-hand sides of equations (1) and (5) and combining terms, it is shown that

$$\left[\frac{(N-1)(km)}{NFt_i}\right]^{(N-1)} = ie^{\left(N-1-NFt_i/(km)\right)} \qquad (6)$$

where t_i is the time corresponding to P_i.

Substituting equation (2) and (6) and taking logarithms, we have

$$\ln i + (N-1)\ln\frac{t_i}{t_{max}} = (N-1)\left[\frac{t_i}{t_{max}} - 1\right] \qquad (7)$$

or

$$N-1 = \frac{\ln i}{\frac{t_i}{t_{max}} - \ln\frac{t_i}{t_{max}} - 1.00} \qquad (8)$$

In addition, equation (2) can be written in the form

$$(km) = \frac{N}{N-1} Ft_{max} \qquad (9)$$

Therefore, equations (8) and (9) can be used to calculate values for the parameters N and (km) if P_{max}, t_{max}, and t_i are known. The value of i is arbitrary as long as it is greater than unity.

In practice, equation (8) was used to calculate N for i equal to 2 and 10. The average of the two values of N was used to characterize the individual curves and to calculate (km). Values of N and (km) were calculated for all of the curves obtained using nitrogen as the carrier gas. The values for krypton are tabulated in the last two columns of Tables I and II, and those for xenon are given in Tables IV, V, and VI. No coherent variation of the values of N with any of the parameters was observed. On the assumption that N is independent of both temperature and flow rate, the average values of N were calculated for each mesh size for each tracer, omitting those values which could be discarded from statistical considerations. These averages varied from 6.9 ± 2.5 for -20+30 mesh charcoal for krypton to 3.3 ± 1.0 for the same mesh for xenon. No variation with charcoal mesh was observed, but the values of N for xenon appear lower than those for krypton.

The values of (km) were calculated using the average values of N for the particular mesh charcoal. The resulting values showed both a temperature and flow rate dependence. The data for krypton using -40+50 mesh charcoal and -20+30 mesh charcoal are plotted in Figures 32 and 33, respectively. The data obtained for xenon using -6+14 mesh charcoal are shown in Figure 34. The krypton data are compared to those calculated for these traps from the work of Browning[2]. All of these curves approach an exponential decrease (with T^{-1}), but the slopes and magnitudes vary considerably with flow rate. The apparent increase of (km) with flow rate is not predicted by theoretical considerations and is an indication of non-equilibrium adsorption conditions in the system.

A comparison of experimental results with the theoretically predicted behavior was made for the data obtained for krypton at $-80^{\circ}C$ using -20+30 mesh charcoal. By using the average value for N of 6.9 for this mesh charcoal and applying the individual values of (km), elution curves were calculated for the four flow rates. These curves are

shown as the smooth plots in Figures 19 through 21, where they are compared to the respective experimental histograms. Since the values of N and (km) used in the calculations were derived from the experimental data, the general agreement in the positions and shapes of the curves is to be expected. However, the magnitudes, or areas under the curves, are not in good agreement, indicating that the basic assumptions involved in their derivation may not be valid.

VI. Discussion

The experimental data for krypton and xenon exhibited the same general pattern. Except for some data at -80°C and a few xenon runs at 0°C, the elapsed times required for quantitative elution of the tracer from the traps were of the order of two minutes or less. In many cases at 100°C, the disappearance times were less than thirty seconds. In these cases, the histogram representing the elution curve consisted of only one or two intervals, since the recorder could not be set for less than eighteen second intervals. Even those curves which extended for several recorder intervals were somewhat insensitive, since the maximum usually occurred at less than half of the disappearance time. This lack of sensitivity is reflected in the values for both the breakthrough and peak times listed in the tables. Values of the breakthrough times could not be determined for krypton at 0° or 100°C or for xenon at 100° because of the very short times involved. Therefore, in composing curves from the experimental data, the breakthrough was taken to be the time required for unobstructed flow from injection manifold to monitor. For sufficiently sensitive curves, experimental values could be determined with varying accuracy. However, it is obvious that breakthrough times could not be used to evaluate the efficiencies of these traps.

Some difficulty was experienced in determining peak times for the runs at higher temperatures and flow rates for the same reasons. However, these values were considered

to be better for correlation of the data than the longer disappearance times because the latter values are a function of the absolute quantity of tracer in a given charge. It is clear that a more sensitive, hence longer, disappearance time will result from a larger charge of tracer. Since the total activities of the runs varied by several factors prior to normalization, the use of the disappearance time was not feasible. Some of the anomolous values for disappearance time in the tables can be attributed to an unusually large or small charge of tracer.

The histograms have the expected skewed-Gaussian shape, normally showing a relatively sharp rise to peak followed by a broader tail. There is no pronounced effect of temperature, flow rate, or particle size on the shape of the elution curves. The curves are significantly displaced in time as flow rate and temperature change. Peak times and disappearance times exhibit a decreasing trend with increasing flow rate. The relationship is not linear as predicted by theory, but the times vary more slowly than the flow. This lack of linearity is reflected in the variations in the calculated values of (km) at constant temperature. This effect may be due to either of two factors, laminar flow or pressure differentials. Laminar flow is important at the flow rates in these experiments and should become greater with increasing flow. Since axial mixing of the gases will also increase with increasing flow, a possible distortion of the tracer charge may occur which would tend to delay the appearance of the peak and to cause the peak time to decrease more slowly than the increase in flow. However, if turbulence were also present, the radial mixing introduced might tend to cancel some of the axial mixing effect.

Substantial pressure differentials were required to maintain the required flow rates through the traps. The pressure drop across the traps varied with flow rate and particle size from about 0.25 atmosphere for coarse charcoal at the lowest flow rate

to about 1.5 atmosphere for the finest charcoal at the fastest flow rate. This change in pressure differential across the trap may have an effect on the adsorption properties of the charcoal and thus may affect the retention time for the tracer. The presence of these "non-ideal" conditions in the system probably leads to non-equilibrium adsorption and thus may preclude agreement between experiment and theory.

The general increase in tracer retention with decreasing temperature is qualitatively in agreement with the observations of Browning[2]. Comparison of the data obtained in this work with those calculated from Browning (see Figures 32 and 33) shows that the values of (km) agree within an order of magnitude, and at higher temperatures the values calculated from Browning fall within the spread of those from this work. However, the slopes of the curves are in poor agreement. It should be noted that the slopes of the curves obtained at the slowest flow rates are in best agreement with Browning's work, and that the agreement becomes less satisfactory as flow rate increases. This behavior probably confirms the previous observation of increasing deviation from equilibrium adsorption conditions with increasing flow rate.

Higher tracer retention efficiency might be expected to accompany decreasing charcoal particle size due to the greater surface areas of the adsorbent. This effect was observed in the peak times for xenon at -6+14 mesh and -20+30 mesh charcoal. However, a comparison of data using -20+30 mesh and -40+50 mesh charcoal shows a reversal of this trend, indicating that -20+30 mesh size is the most efficient of the three meshes. Several possible factors may be affecting these results. First, at the end of the tests, the -40+50 mesh charcoal was observed to have been compacted in the trap so that its length was decreased by about one inch. While this effect might tend to reduce the retention times proportionately, it would not appear to be of sufficient magnitude to account for the entire effect. Also, the pressure differential required to

maintain a given flow rate through this mesh charcoal was about 25 percent greater than for -20+30 mesh. The change in pressure differential may affect the adsorptive behavior of the gases and cause the traps to be less efficient. Another effect which may negate the increase in surface area and collision probability is an increase in linear flow rate through the trap as the particle size is reduced. Since the charcoal particles are not spherical in shape, they can become more closely packed as their size diminishes. Consequently, the free volume available for gas flow decreases. While this effect will increase the collision probability between gas particles and adsorbent, it also increases the linear rate of flow through the trap itself since the adsorbent bed is effectively a constriction in the flow system. The increase in flow would be accompanied by an increase in turbulence, introducing another parameter. It is not feasible to evaluate the net effect of these several factors quantitatively. However, it is possible that they may combine in such a manner as to cause a greater deviation from equilibrium adsorption conditions and thus decrease the retention efficiency of a trap as the particle size decreases.

Such a combination of parameters is not necessarily in conflict with the fact that -20+30 mesh charcoal retains xenon longer than -6+14 mesh. The coarser mesh size represents an appreciable fraction of the trap diameter. Hence, the possibility of channeled flow past fairly long sections of the adsorbent bed exists. Browning[2] has observed in experiments with horizontal beds that a settling effect yielding a 3 percent void volume decreases the breakthrough time by more than 80 percent and the peak time by more than 15 percent. Therefore, a reduction in retention efficiency for -6+14 mesh charcoal may well result from a distribution of discontinuous channels throughout the charcoal bed.

No detectable change was observed when dry air was substituted for nitrogen as the carrier gas. The peaks of the corresponding histograms show general agreement

within one recorder interval. The variations in the shapes of these histograms are reasonably representative of those of duplicate measurements at the several experimental conditions. These variations are representative of the general agreement of duplicate experiments throughout this work. The dispersions probably are due to two principal factors. One of these involves the use of histograms to characterize the elution patterns. A shift of the peak time of only a few percent can readily cause the peak of a histogram to shift one recorder interval. A more fundamental effect involves a possible perturbation of flow rates and pressure differentials at injection time. Even though the system was designed to minimize these perturbations, changing the flow from the bypass to the injection manifold may produce a temporary change in pressure differential at the time of injection. Since the times required for passage of the tracer through the traps were very short, they may be comparable in duration to the time required for recovery of equilibrium pressure across the trap from any possible perturbation. While precautions were taken to minimize pressure excursions, their occurrence in a non-reproducible fashion cannot be excluded, and they may affect the precision of the experimental data.

The foregoing discussion has been concerned primarily with the general behavior of xenon and krypton under the several sets of experimental conditions. While the trends observed with both tracers were qualitatively similar, the absolute retention efficiencies are distinctly different. Comparison of the data for -40+50 mesh charcoal in Tables I and IV and for -20+30 mesh charcoal in Tables II and V shows that the retention times for xenon are as much as an order of magnitude greater than those for krypton at the same temperature and flow rate. The values diverge with decreasing temperature. The larger retention efficiency for xenon is also reflected in significantly larger values of (km), especially at lower temperatures. Browning[2] has also observed that the peak time for krypton release occurs at about 10 percent of that for xenon. This behavior

was expected from the values of the isotherms for adsorption of pure xenon and pure krypton on charcoal in a static system.

Several of the values in the tables and a number of the histograms in the figures are not in accord with these general observations. These discrepancies were repeated and confirmed. They may be attributed to combinations of the experimental difficulties and "non-ideal" conditions which have already been discussed.

The calculated values for the number of theoretical chambers in the individual traps have a rather large uncertainty since the values calculated using the two values of i frequently differed greatly. This uncertainty results from the relationship between N and the shape of the elution curve. Since for many of the histograms the corresponding curve had to be selected arbitrarily, the N values showed considerable dispersion. However, N appears constant within experimental error for the several flow rates, temperatures, and particle sizes for each tracer. If N is truly independent of temperature and flow rate, the standard deviations of the average values given in the tables are representative of the errors in the calculated values. These deviations ranged from about 30 percent to nearly 70 percent of the value of N. The values of N for xenon appear to be consistently lower than those for krypton, but the significance of this difference is doubtful. The data of Browning and Bolta[1] indicated that N for Kr^{85} in the presence of nitrogen carrier was independent of temperatures between -110°C and +16°C. However, Browning[2] has also obtained a variation of N for Kr^{85} in the presence of oxygen carrier at temperatures between 25°C and 100°C. Although the data in this report exclude a strong temperature dependence for N, they cannot exclude the presence of a small effect.

The apparent dependence of the adsorption capacity of the traps on both temperature and flow rate has already been discussed. It has been deduced that the test

conditions in this work preclude the attainment of equilibrium conditions and, therefore, render the basic assumptions of the correlative method invalid. The theoretical peak time is determined by the value of (km) for the corresponding experimental curve. Since (km) is, in the first approximation, directly proportional to the experimental value of t_{max}, a reasonably good agreement between the experimental and theoretical values must follow. In order to establish a significant correlation, it is required that the shapes and magnitudes of the curves coincide. This has not been observed in this work, partially because of the insensitive measure of N. However, in view of the evidence presented for non-ideal or non-equilibrium conditions in the traps, the lack of agreement between theory and experiment is not surprising.

VII. Conclusions

The experimental data obtained in this program lead to the following observations:

1. These traps have low retention efficiencies for both xenon and krypton at the particular test conditions studied.

2. The retention efficiency for xenon on charcoal traps is greater than that for krypton under the same conditions. The ratio of the peak times and consequently of (km) varied from a factor of ten at -80°C to about a factor of two at 100°C. The ratio should approach unity near zero adsorption conditions.

3. At constant flow rate and particle size, the retention efficiency for both tracers increases with decreasing temperature. However, the efficiency for xenon increases more rapidly. At 100°C, the possibility of a significant fraction of the tracer passing through the trap without adsorption cannot be excluded by these data.

4. At constant temperature and particle size, the retention efficiency for xenon and krypton decreases with increasing flow rate. However, the peak time varies more slowly than the flow rate. This straggling tendency has been attributed, in part, to

the expected increase in axial mixing of the gases with increasing flow rate.

5. At constant temperature and flow rate, -20+30 mesh charcoal appears more efficient than either the coarser or the finer mesh. The poorer efficiency of the -6+14 mesh bed has been attributed to local, discontinuous channeling. The decrease in efficiency at -40+50 mesh may be due to the strong increase in linear flow rate in the constricted areas overriding the higher collision probability and surface area of the trap.

6. There is no detectable difference in retention efficiency for krypton upon changing the carrier gas from nitrogen to dry air.

7. Adsorbed iodine is retained quantitatively by these traps at temperatures up to 100°C and integrated nitrogen flows of greater than 300 ft^3. Since no appreciable movement of the tracer was detected under these limiting conditions, it appears that the traps can be considered to have 100 percent efficiency for iodine for much larger total flows at these temperatures.

An attempt to correlate these data using a modification of the method of Browning and Bolta[1] leads to the following conclusions:

1. The calculated number of theoretical chambers in the traps appears constant, within experimental error, for all conditions for a given tracer. Uncertainties of from 30 to 70 percent in the values of N preclude observation of slight variations with any parameter.

2. Values of N for xenon are consistently lower than for krypton under the same conditions, but the differential appears to be within experimental error.

3. The tendency of (km) to increase with increasing flow rate indicates the occurrence of a non-equilibrium process in the traps. This deviation from ideal behavior is probably due to laminar or turbulent flow conditions or variable pressure differentials in the system.

4. The adsorption capacity of the traps, (km), decreases exponentially with increasing temperature. The temperature dependence is not in quantitative agreement with that observed by Browning[2]. However, the slopes of the curves obtained using the lower flow rates approach more closely to that of Browning confirming the relationship between higher flows and non-equilibrium adsorption conditions in the traps.

5. In summary, quantitative agreement between experimental and theoretical elution curves has not been found.

These data comprise a body of information for retention of xenon and krypton by charcoal traps at flow rates of interest in engineering applications. However, the trap sizes used here were relatively small for handling large volumes of gas. Therefore, it appears desirable to be able to extend these data to longer traps or traps having different geometries. However, in view of the lack of precise information on the deviation of retention efficiencies from theoretical behavior, these data cannot be extrapolated, with confidence, to larger traps or to different trap temperatures or flow conditions. Therefore, additional investigations of the phenomenology of rare gas retention by charcoal in dynamic systems are indicated.

(1) W. E. Browning and C. C. Bolta, USAEC Report No. ORNL-2116 (1956).

(2) W. E. Browning, private communication.

TABLE I

Retention of Krypton by -40+50 Mesh Charcoal in the Presence of Nitrogen Carrier Gas

Trap Temp. (°C)	Flow Rate (ft/min)	Breakthrough Time[a] (sec)	Peak Time[a] (sec)	Disappearance Time[a] (sec)	N	km (cm^3)
-80	40	40	139	288	15	2.7×10^3
-80	80	16	65	155	9.9	2.8×10^3
-80	160	9.6	27	69	8.4	2.1×10^3
-80	300	15	43	72	11.4	6.3×10^3
0	40	~0[b]	13.5	85	2.5	2.6×10^2
0	80	~0[b]	7.6	57	2.6	3.0×10^2
0	160	~0[b]	12.0	57	3.4	9.5×10^2
0	300	~0[b]	15.0	51	3.7	22×10^2
100	40	~4.5[b]	19.5	94	5.4	3.9×10^2
100	80	~0[b]	10.2	65	3.0	4.0×10^2
100	160	~0[b]	6.6	52	2.6	5.2×10^2
100	300	~0[b]	7.2	48	2.8	11×10^2

Average 5.9 ± 3.5

[a] Elapsed time corrected for flow time through system

[b] Estimated from histogram

TABLE II

Retention of Krypton by -20+30 Mesh Charcoal in the Presence of Nitrogen Carrier Gas

Trap Temp. (°C)	Flow Rate (ft/min)	Breakthrough Time[a] (sec)	Peak Time[a] (sec)	Disappearance Time[a] (sec)	N	km (cm^3)
-80	40	36	178	571	29	3.4×10^3
-80	80	4.5	99	353	6.6	3.8×10^3
-80	160	<7[b]	60	157	2.3	4.6×10^3
-80	300	<3[b]	43	153	5.3	6.2×10^3
0	40	~0[d]	8.0	41	2.8	1.5×10^2
0	80	~0[d]	10.2	33	8.4	3.9×10^2
0	160	~0[d]	10.6	34	9.3	8.1×10^2
0	300	~0[d]	9.0	19	9.6	13.0×10^2
100	40	~0[d]	3.2	5	3.7	0.6×10^2
100	80	~0[d]	5.7	<11[b]	8.8	2.2×10^2
100	160	~0[d]	6.3	<14[b]	12.4	4.8×10^2
100	300	~0[d]	4.0	< 8[c]	7.0	5.8×10^2

Average 6.9 ± 2.5

[a] Elapsed time corrected for flow time through system.

[b] Upper limit estimated from histogram.

[c] Upper limit estimated during operation.

[d] Estimated from histogram.

TABLE III

Effect of Carrier Gas on Retention of Krypton by Charcoal at -80°C

Flow Rate (ft/min)	Charcoal Mesh	Carrier Gas	Breakthrough Time[a] (sec)	Peak Time[a] (sec)	Disappearance Time[a] (sec)
40	-20+30	N_2	36	178	517
40	-20+30	Dry Air	36	200	525
40	-40+50	N_2	40	139	288
40	-40+50	Dry Air	49	130	320
80	-20+30	N_2	4.5	99	335
80	-20+30	Dry Air	4.0	87	335
80	-40+50	N_2	16	65	155
80	-40+50	Dry Air	36	85	170

[a] Elapsed time corrected for system flow time.

TABLE IV

Retention of Xenon by -40+50 Mesh Charcoal in the Presence of Nitrogen Carrier Gas

Trap Temp. (°C)	Flow Rate (ft/min)	Breakthrough Time[a] (sec)	Peak Time[a] (sec)	Disappearance Time[a] (sec)	N	km (cm^3)
0	40	134	224	460	42	4.9×10^3
0	80	47	116	280	10.9	5.0×10^3
0	160	~0[b]	46	174	1.7	4.0×10^3
100	40	~0[b]	20	76	6.1	4.3×10^2
100	80	~0[b]	15	60	1.6	6.5×10^2
100	160	~0[b]	7.2	50	1.9	6.2×10^2
100	300	~0[b]	9.0	77	2.6	13×10^2

Average 4.1 ± 2.8

[a] Elapsed time corrected for flow time through system.

[b] Estimated from histogram.

TABLE V

Retention of Xenon by -20+30 Mesh Charcoal
in the Presence of Nitrogen Carrier Gas

Trap Temp. (°C)	Flow Rate (ft/min)	Breakthrough Time[a] (sec)	Peak Time[a] (sec)	Disappearance Time[a] (sec)	N	km (cm^3)
0	80	~10[b]	80	590	3.0	3.8×10^3
100	40	~0[b]	15	130	2.5	3.5×10^2
100	80	~0[b]	17	102	3.9	8.0×10^2
100	160	~0[b]	16	88	2.0	15×10^2
100	300	~0[b]	18	88	5.1	17×10^2

Average 3.3 ± 1.0

[a] Elapsed time corrected for flow time through system.

[b] Estimated from histogram.

TABLE VI

Retention of Xenon by -6+14 Mesh Charcoal
in the Presence of Nitrogen Carrier Gas

Trap Temp. (°C)	Flow Rate (ft/min)	Breakthrough Time[a] (sec)	Peak Time[a] (sec)	Disappearance Time[a] (sec)	N	km (cm^3)
-80	80	101	548	---	21	2.5×10^4
0	40	<10	80	880	7.8	1.8×10^3
0	80	<10	70	1070	4.0	3.2×10^3
0	160	<5	33	660	2.5	3.0×10^3
100	40	~0[b]	2.7	15	3.1	0.6×10^2
100	80	~0[b]	9.2	37	1.9	4.2×10^2
100	160	~0[b]	6.7	23	2.4	6.2×10^2
100	300	~0[b]	6.4	21	2.5	11×10^2
				Average	3.5 ± 1.4	

[a] Elapsed time corrected for flow time through system.

[b] Estimated from histogram.

TABLE VII

Retention of Iodine by Charcoal in
the Presence of Nitrogen Carrier Gas

Charcoal Mesh	Trap Temp. (°C)	Flow Rate (ft/min)	Time of Test (hr.)	Volume of Nitrogen Passed Through Trap (ft^3)	Result
-20+30	-80	40	18.3	38.4	No detectable movement of adsorbed iodine
-20+30	-80	300	5.1	80.1	No detectable movement of adsorbed iodine
-6+14	100	300	20.1	316	No detectable movement of adsorbed iodine

FIGURE 1
EXPERIMENTAL APPARATUS

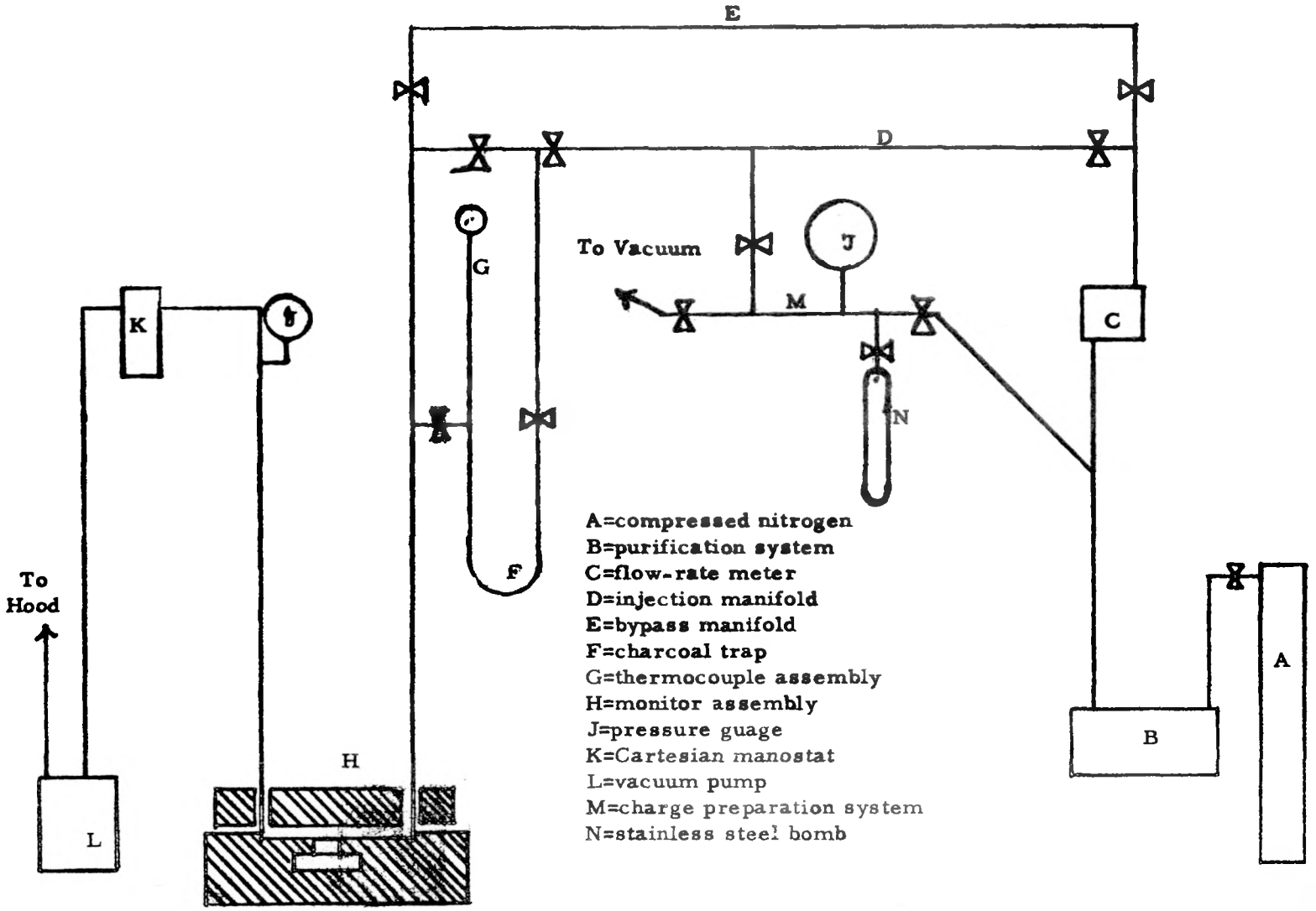

FIGURE 2
CHARGING AND TRAPPING SYSTEM FOR IODINE EXPERIMENTS

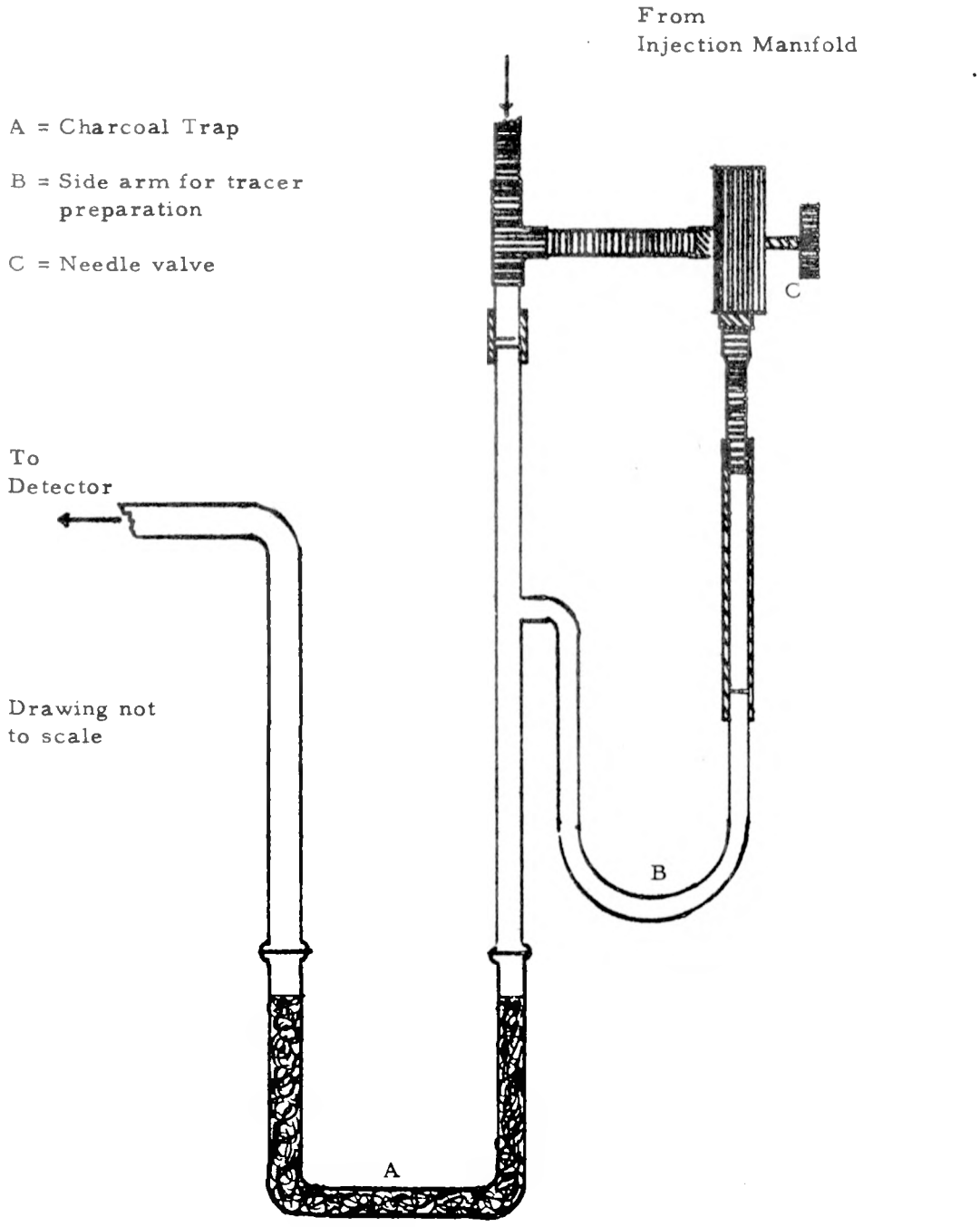

FIGURE 3
EFFECT OF FLOW RATE ON RETENTION OF KRYPTON BY
-40+50 MESH CHARCOAL AT 100°C

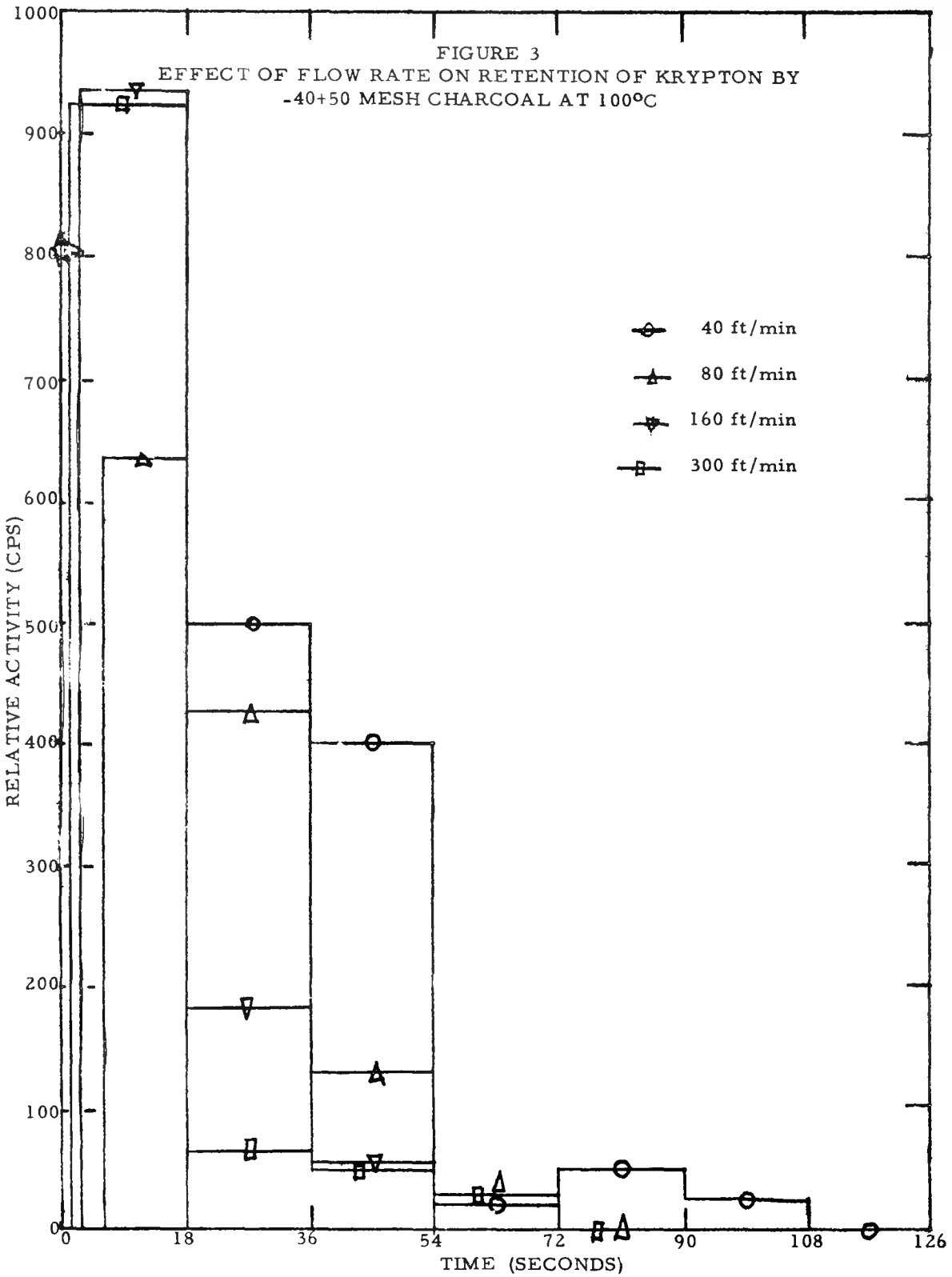

FIGURE 4
EFFECT OF FLOW RATE ON RETENTION OF KRYPTON BY
-40+50 MESH CHARCOAL AT 0°C

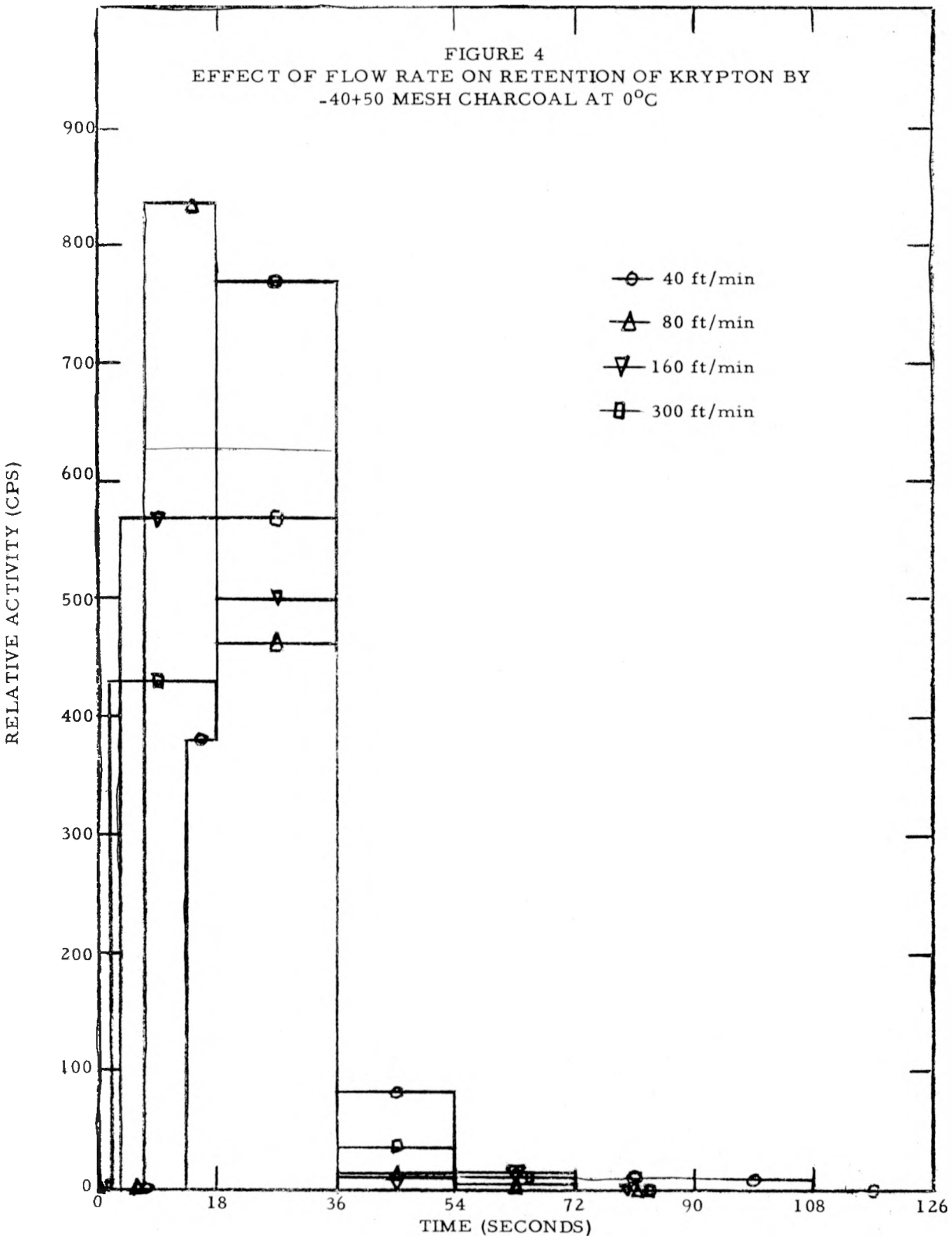

FIGURE 5

EFFECT OF FLOW RATE ON RETENTION OF KRYPTON BY -40+50 MESH CHARCOAL AT -80°C

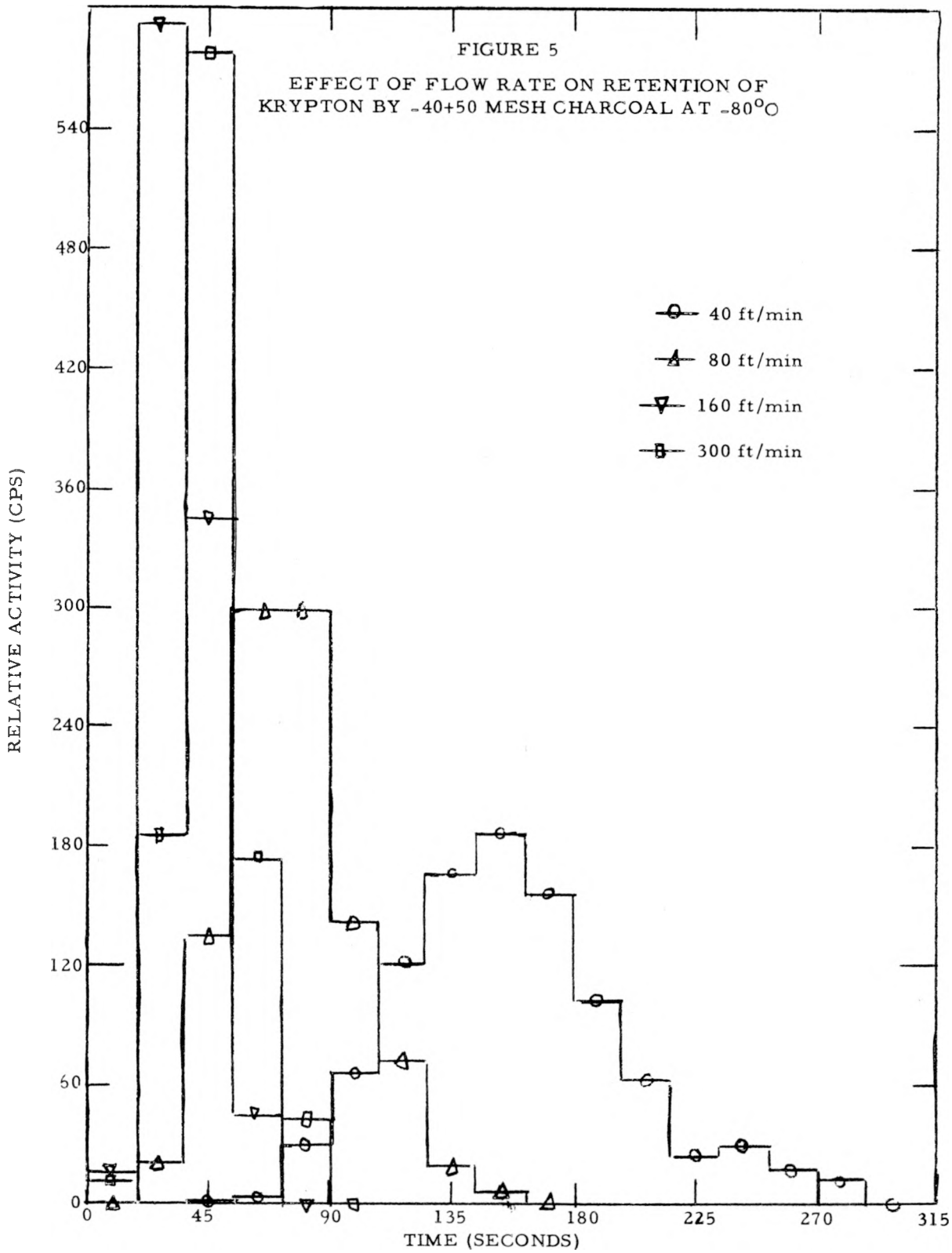

FIGURE 6
EFFECT OF TEMPERATURE ON RETENTION OF KRYPTON BY
-40+50 MESH CHARCOAL AT 40 FT/MIN FLOW RATE

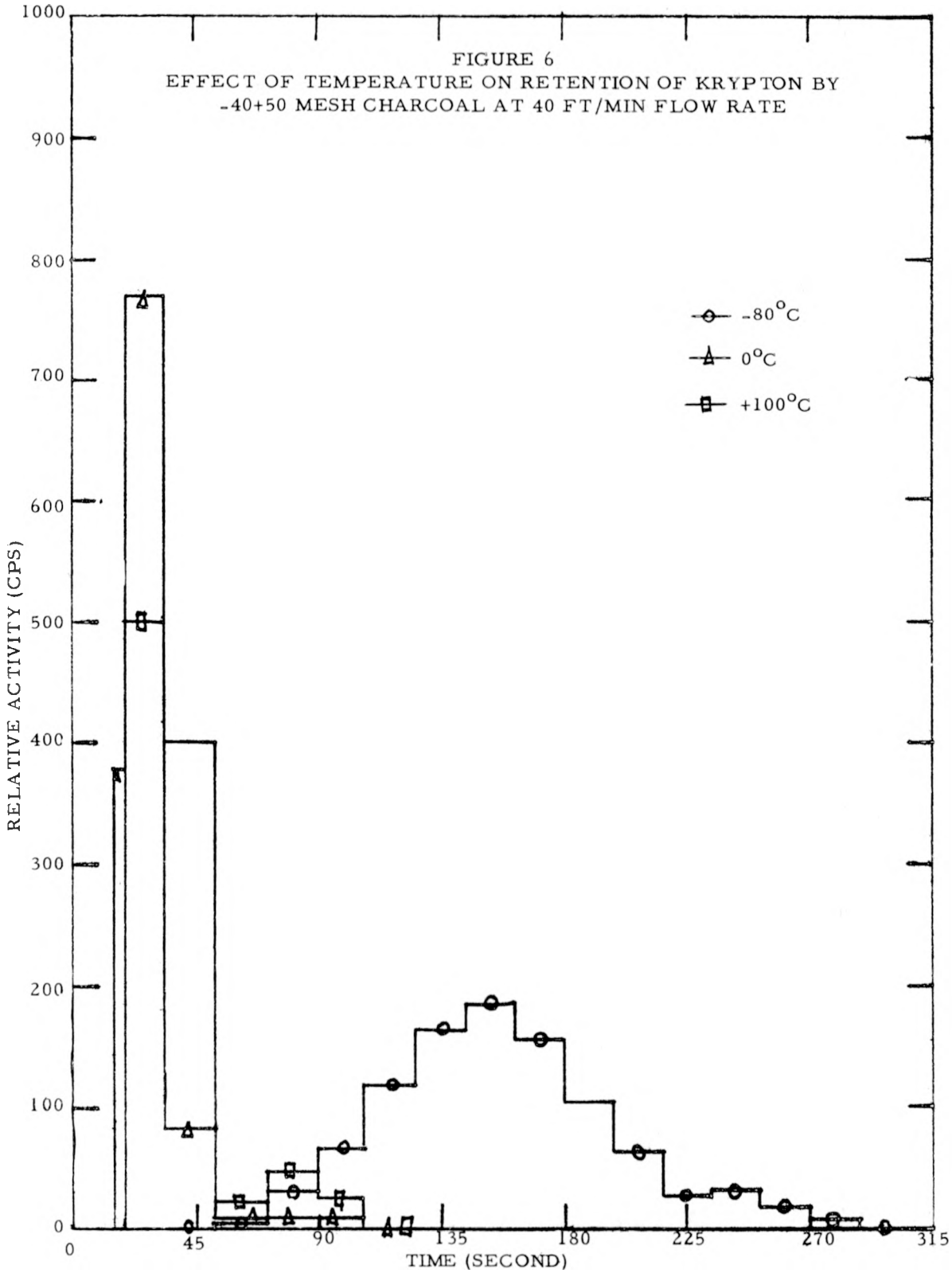

FIGURE 7
EFFECT OF TEMPERATURE ON RETENTION OF KRYPTON BY
-40+50 MESH CHARCOAL AT 80 FT/MIN FLOW RATE

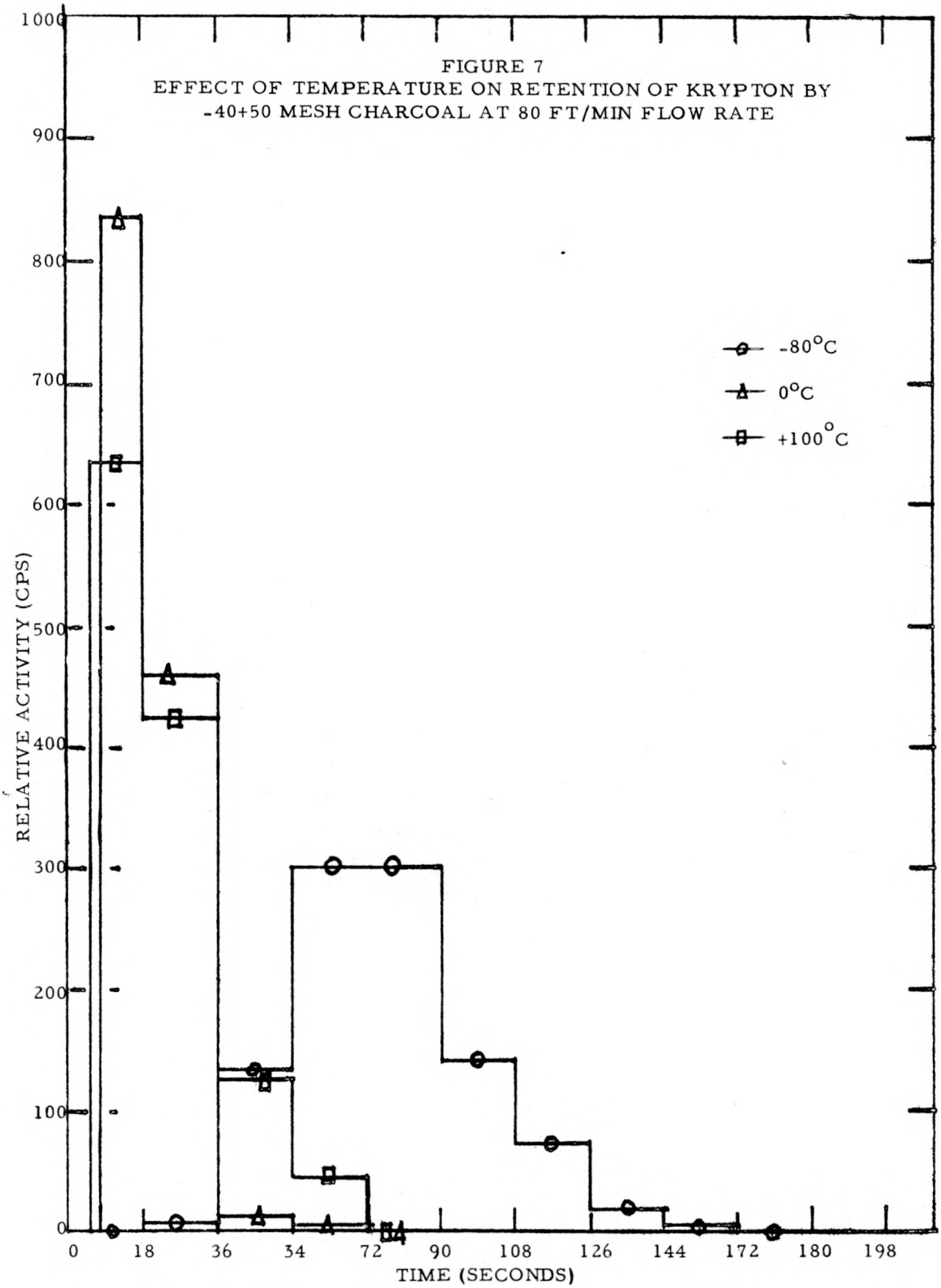

FIGURE 8
EFFECT OF TEMPERATURE ON RETENTION OF KRYPTON BY -40+50 MESH CHARCOAL AT 160 FT/MIN FLOW RATE

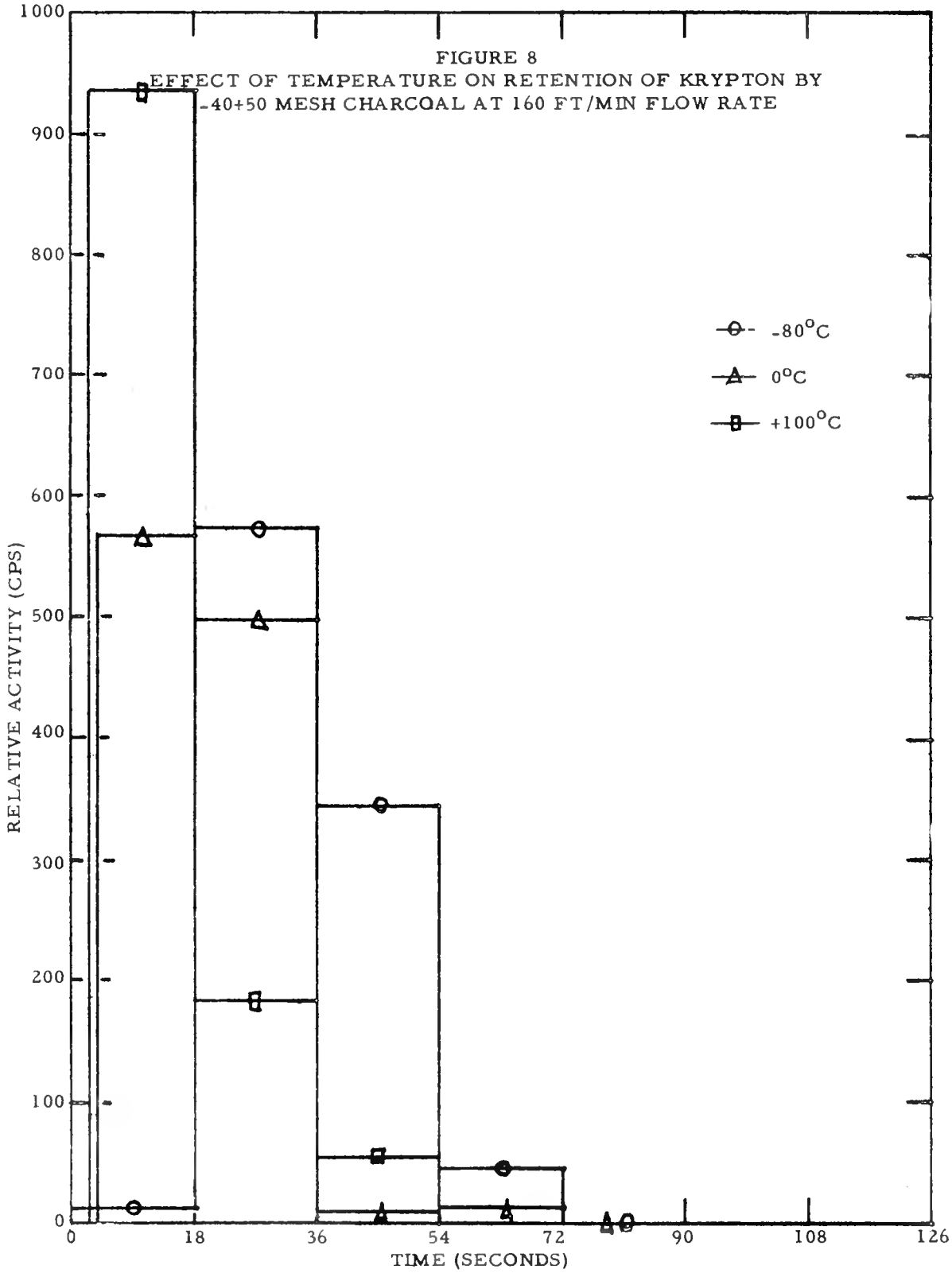

FIGURE 9
EFFECT OF TEMPERATURE ON RETENTION OF KRYPTON BY -40+50 MESH CHARCOAL AT 300 FT/MIN FLOW RATE

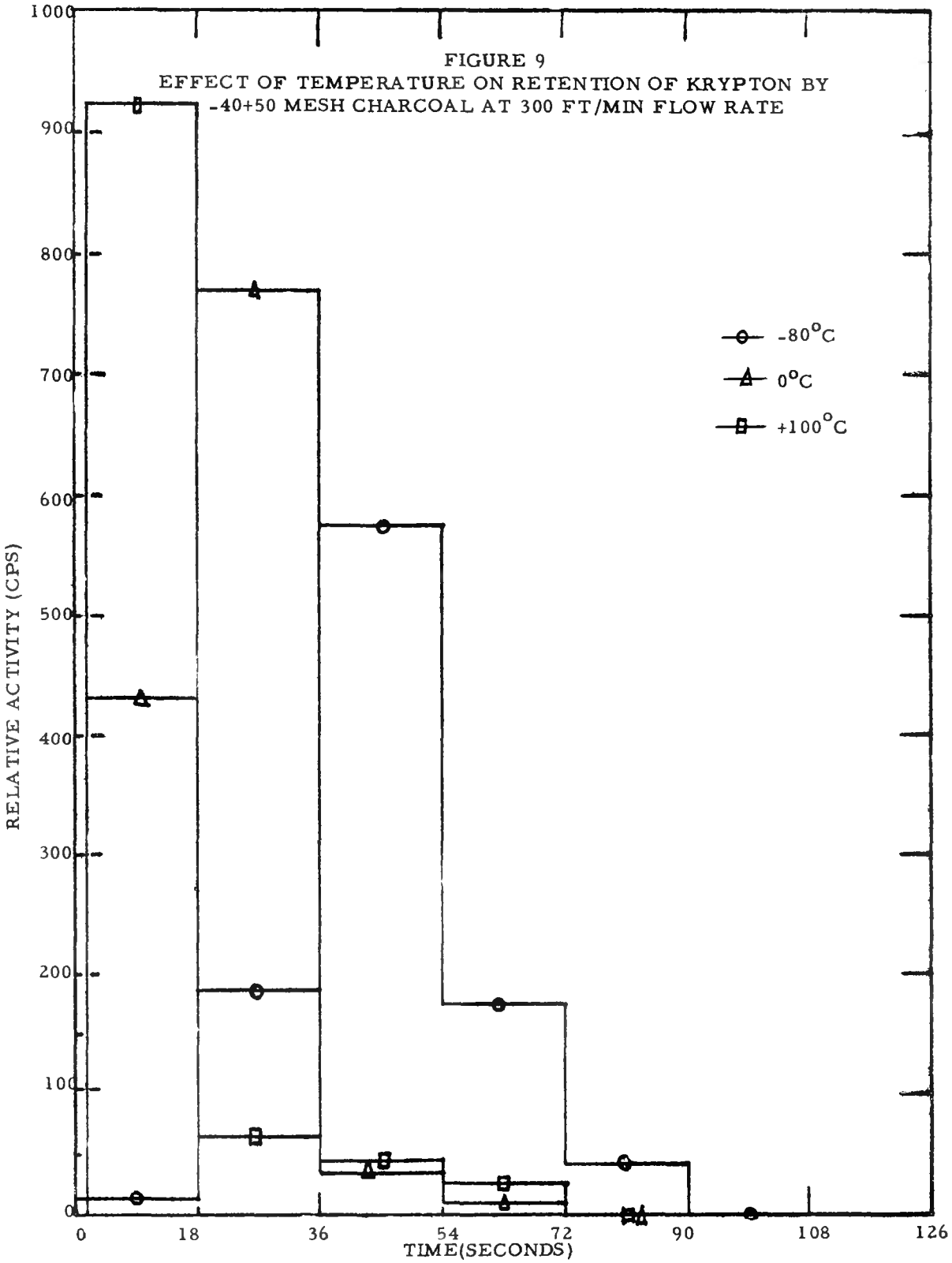

FIGURE 10
EFFECT OF FLOW RATE ON
RETENTION OF KRYPTON BY
-20+30 MESH CHARCOAL AT 100°C

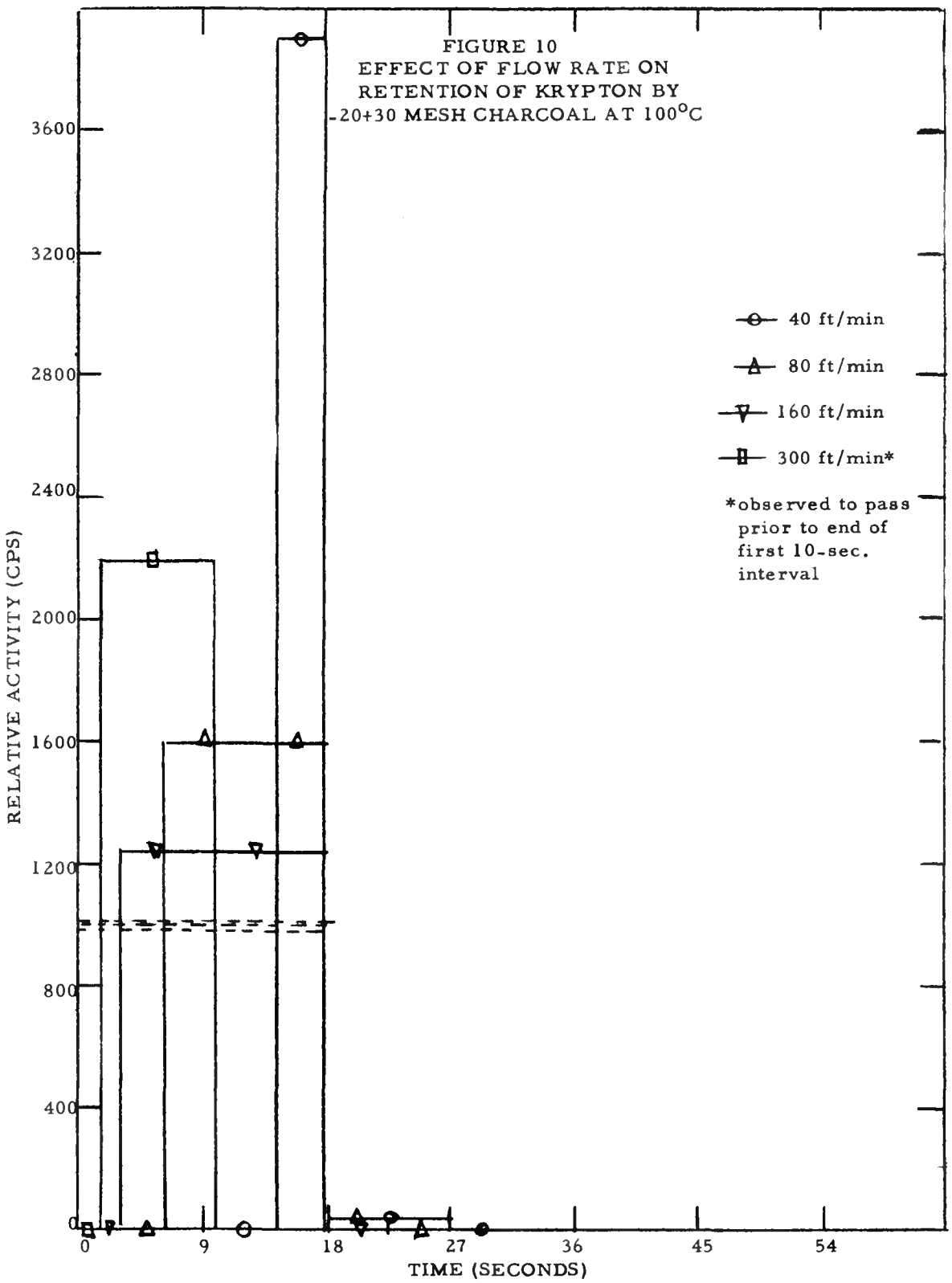

FIGURE 11
EFFECT OF FLOW RATE ON RETENTION OF KRYPTON BY
-20+30 MESH CHARCOAL AT 0°C

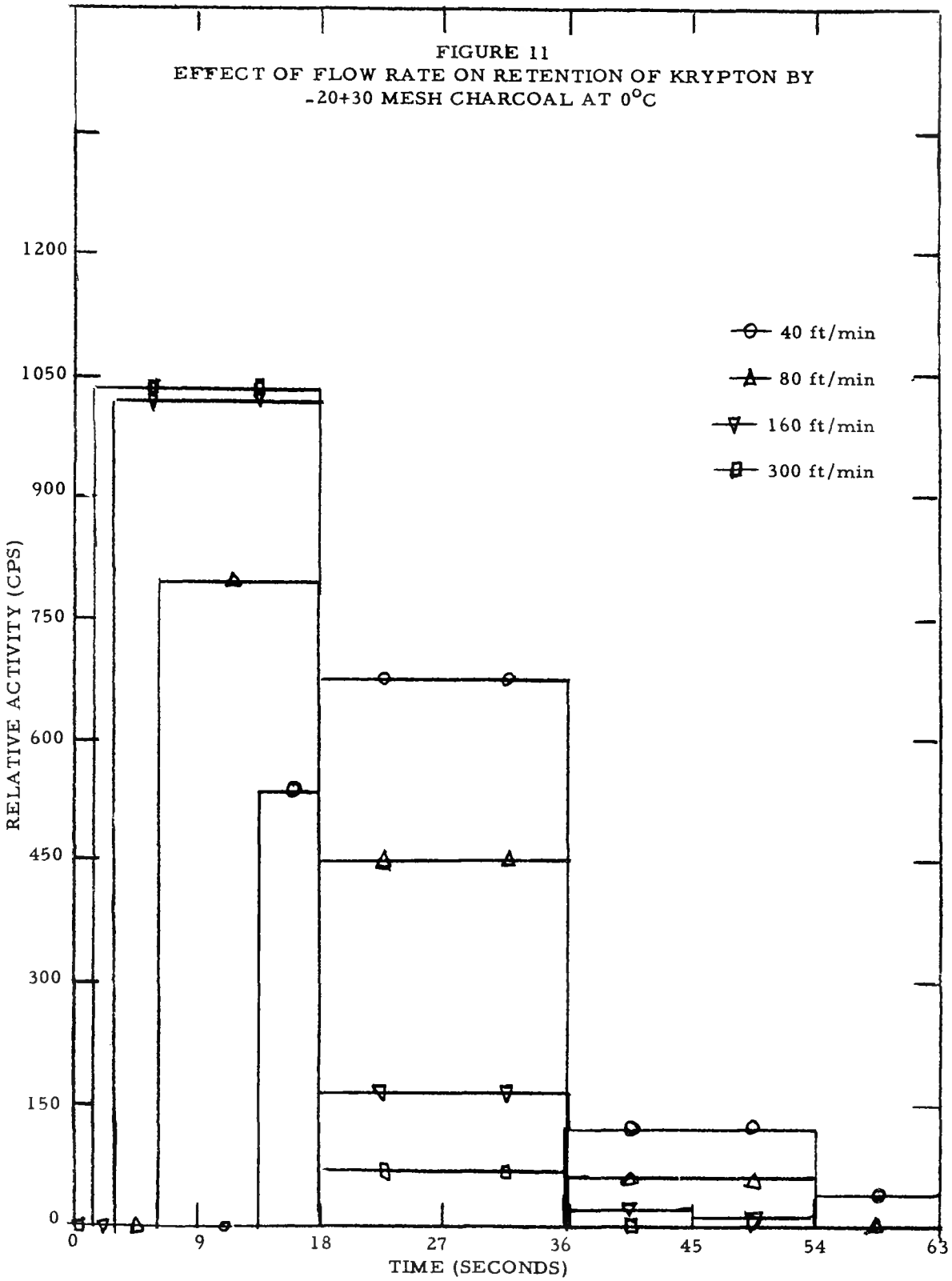

FIGURE 12
EFFECT OF FLOW RATE ON RETENTION OF KRYPTON BY
-20+30 MESH CHARCOAL AT -80°C

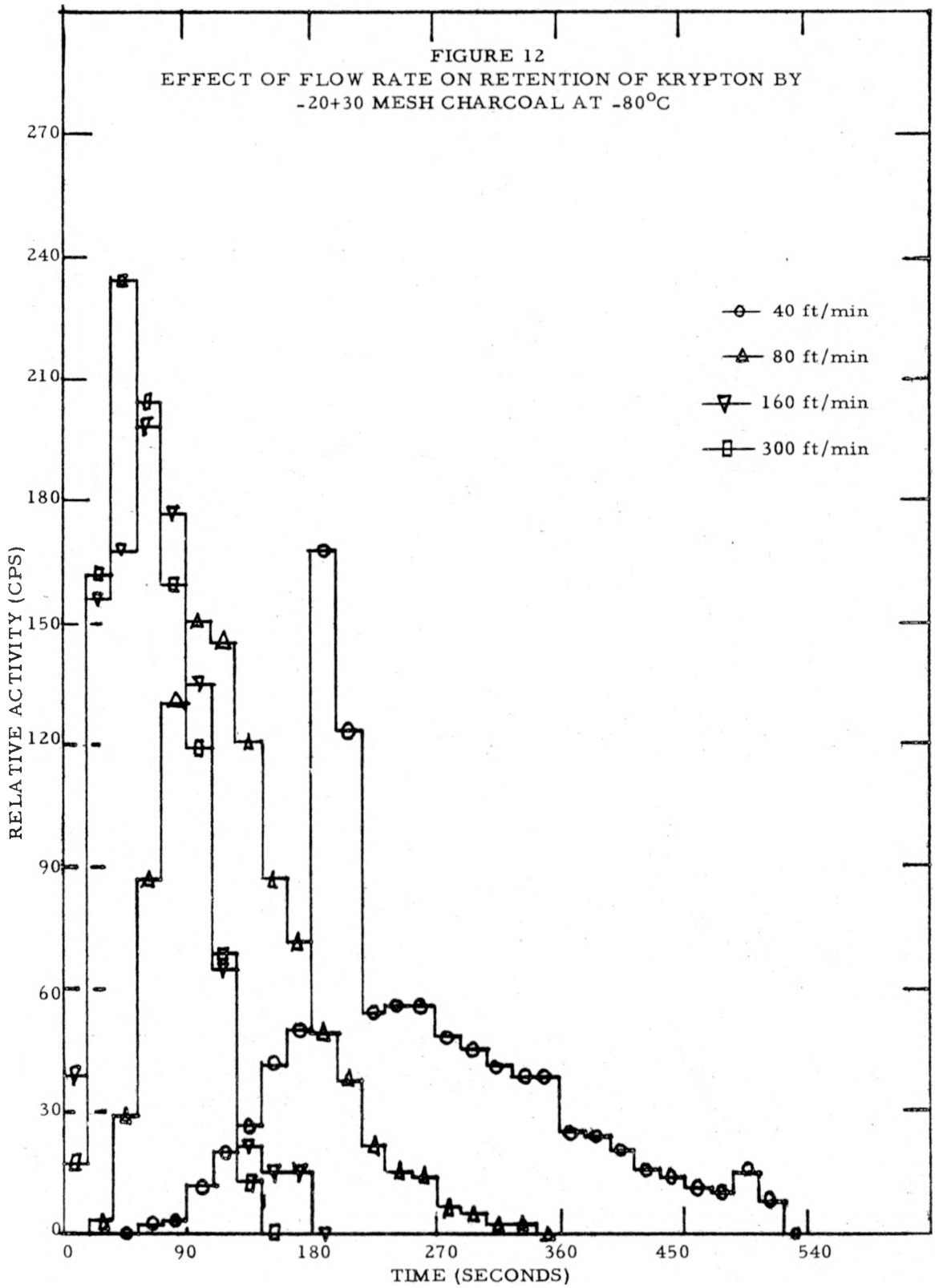

FIGURE 13
EFFECT OF TEMPERATURE ON RETENTION OF KRYPTON BY
-20+30 MESH CHARCOAL AT 40 FT/MIN FLOW RATE

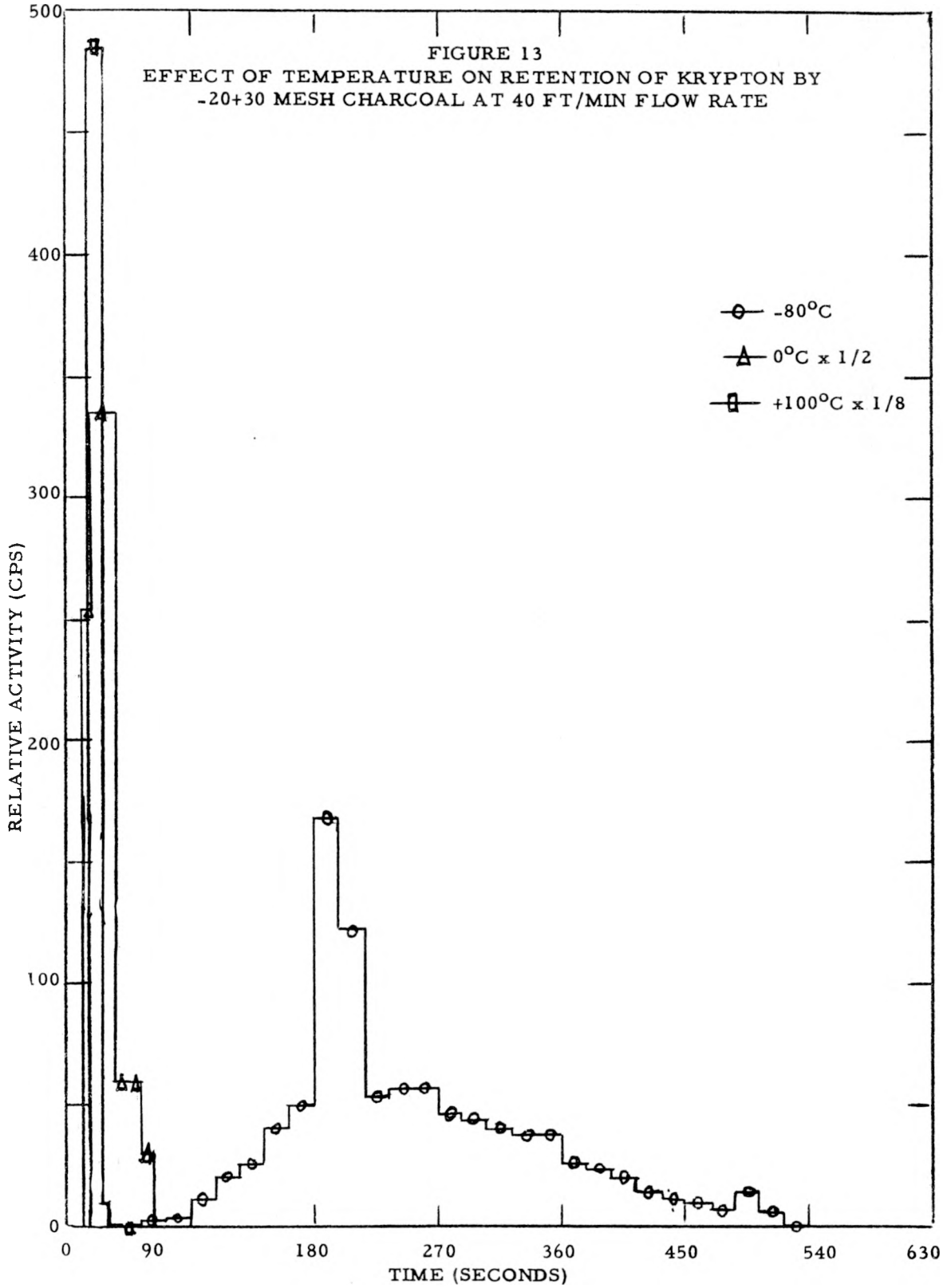

FIGURE 14
EFFECT OF TEMPERATURE ON RETENTION OF KRYPTON BY
-20+30 MESH CHARCOAL AT 80 FT/MIN FLOW RATE

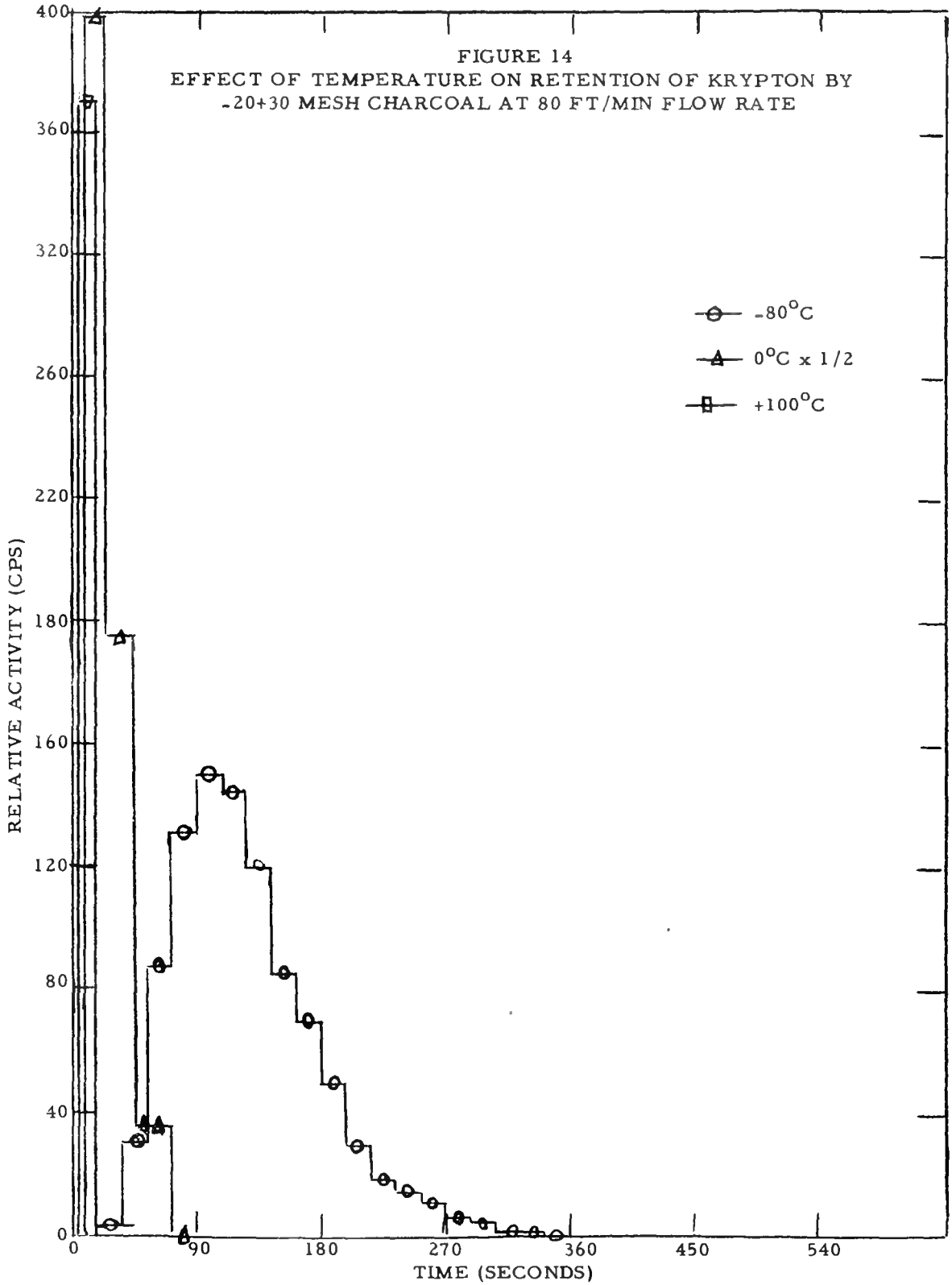

FIGURE 15
EFFECT OF TEMPERATURE ON RETENTION OF KRYPTON BY
-20+30 MESH CHARCOAL AT 160 FT/MIN FLOW RATE

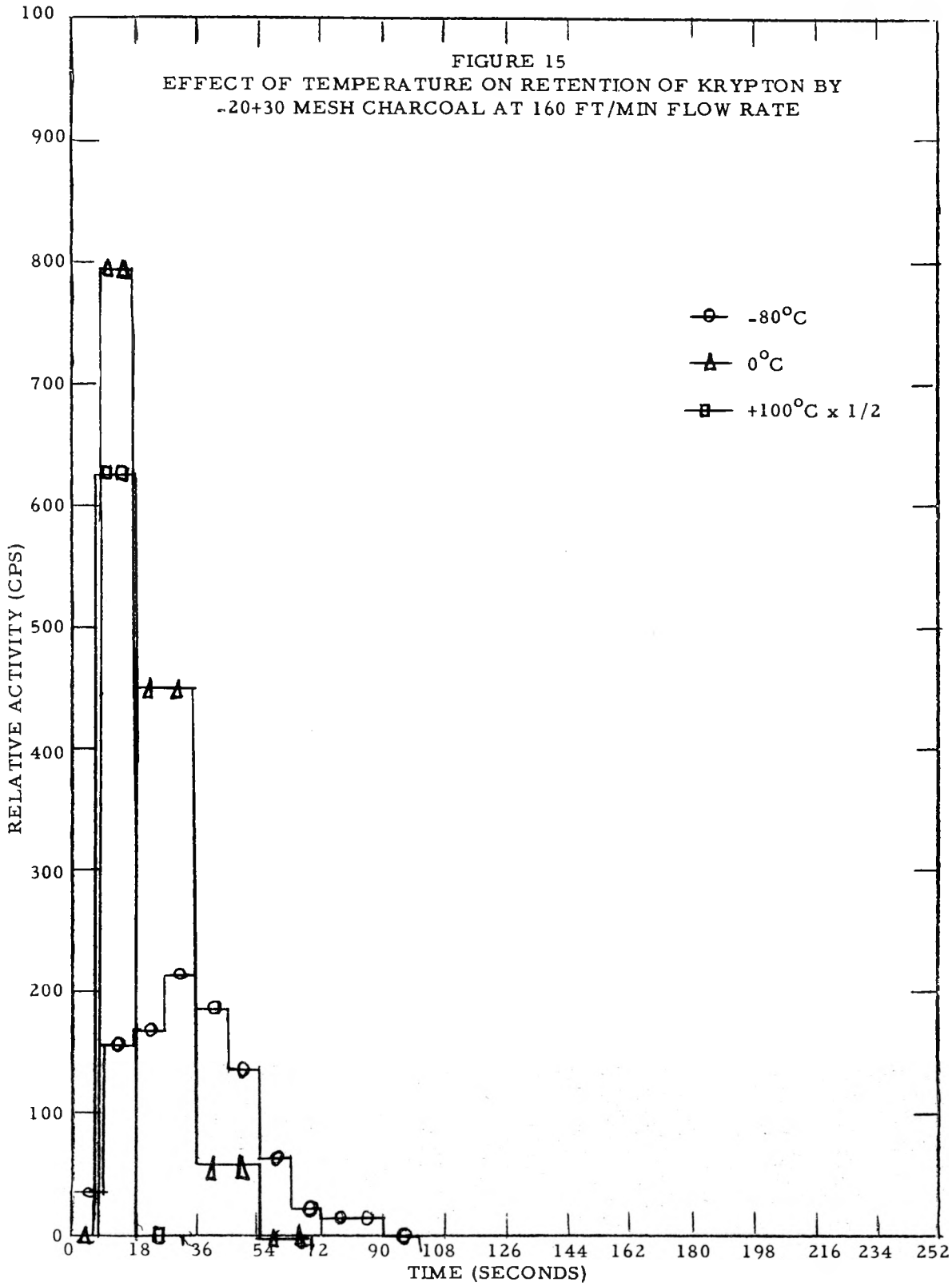

FIGURE 16
EFFECT OF TEMPERATURE ON RETENTION OF KRYPTON BY
-20+30 MESH CHARCOAL AT 300 FT/MIN FLOW RATE

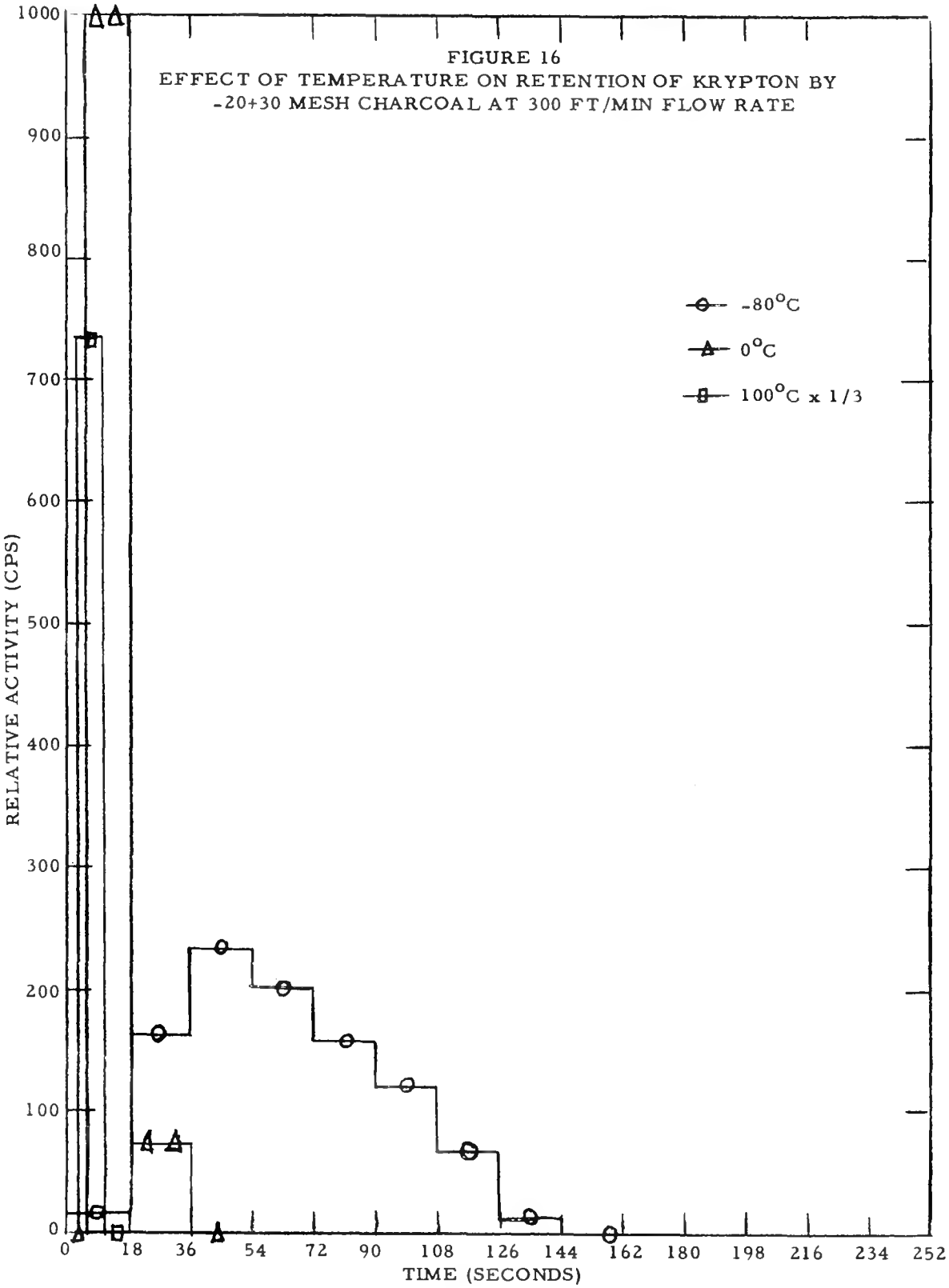

FIGURE 17

EFFECT OF CARRIER GAS COMPOSITION ON RETENTION OF KRYPTON BY -40+50 MESH CHARCOAL AT -80°C AND 40 FT/MIN FLOW RATE

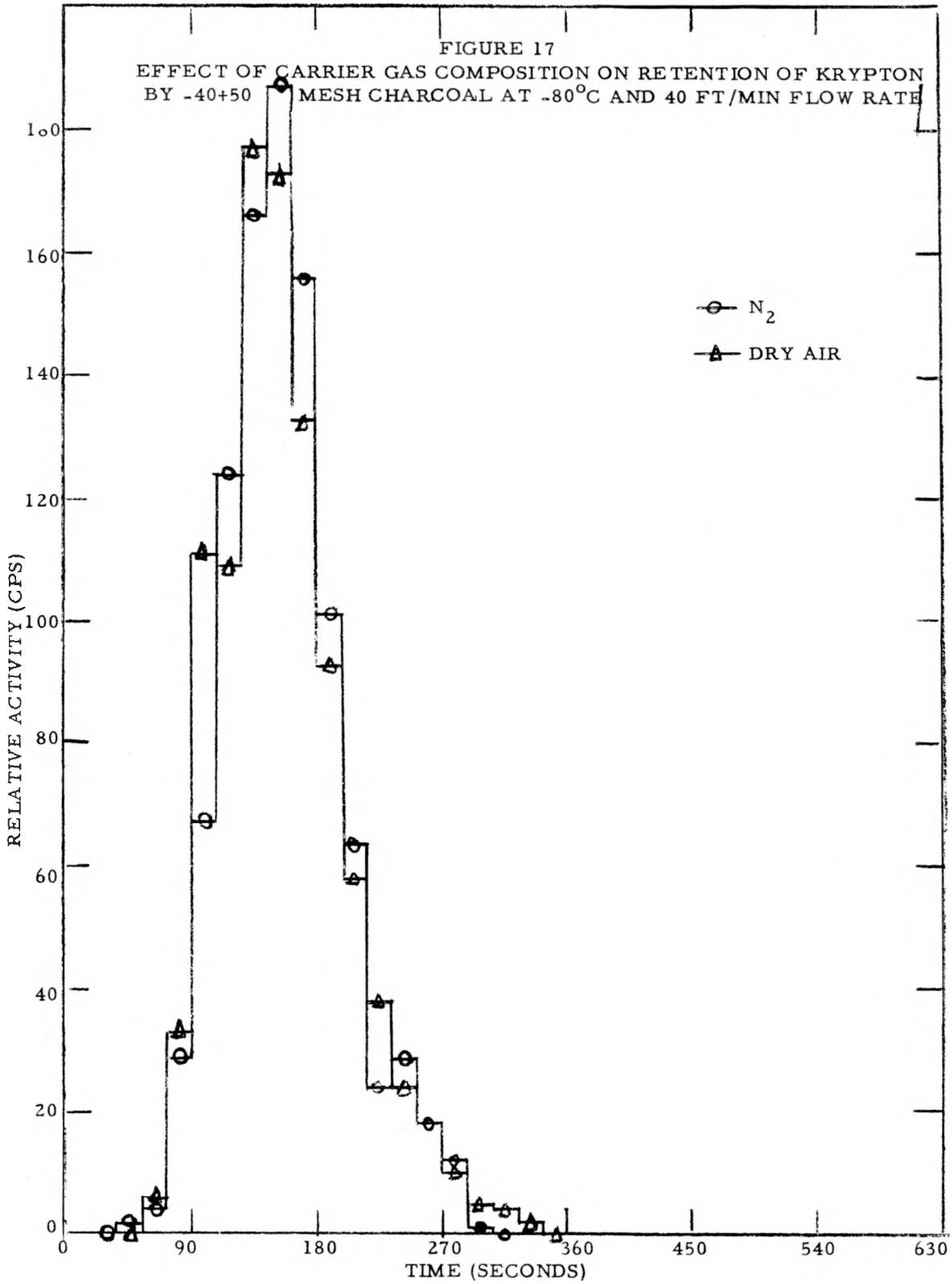

FIGURE 18
EFFECT OF CARRIER GAS COMPOSITION ON RETENTION OF KRYPTON BY -40+50 MESH CHARCOAL AT -80°C AND 80 FT/MIN FLOW RATE

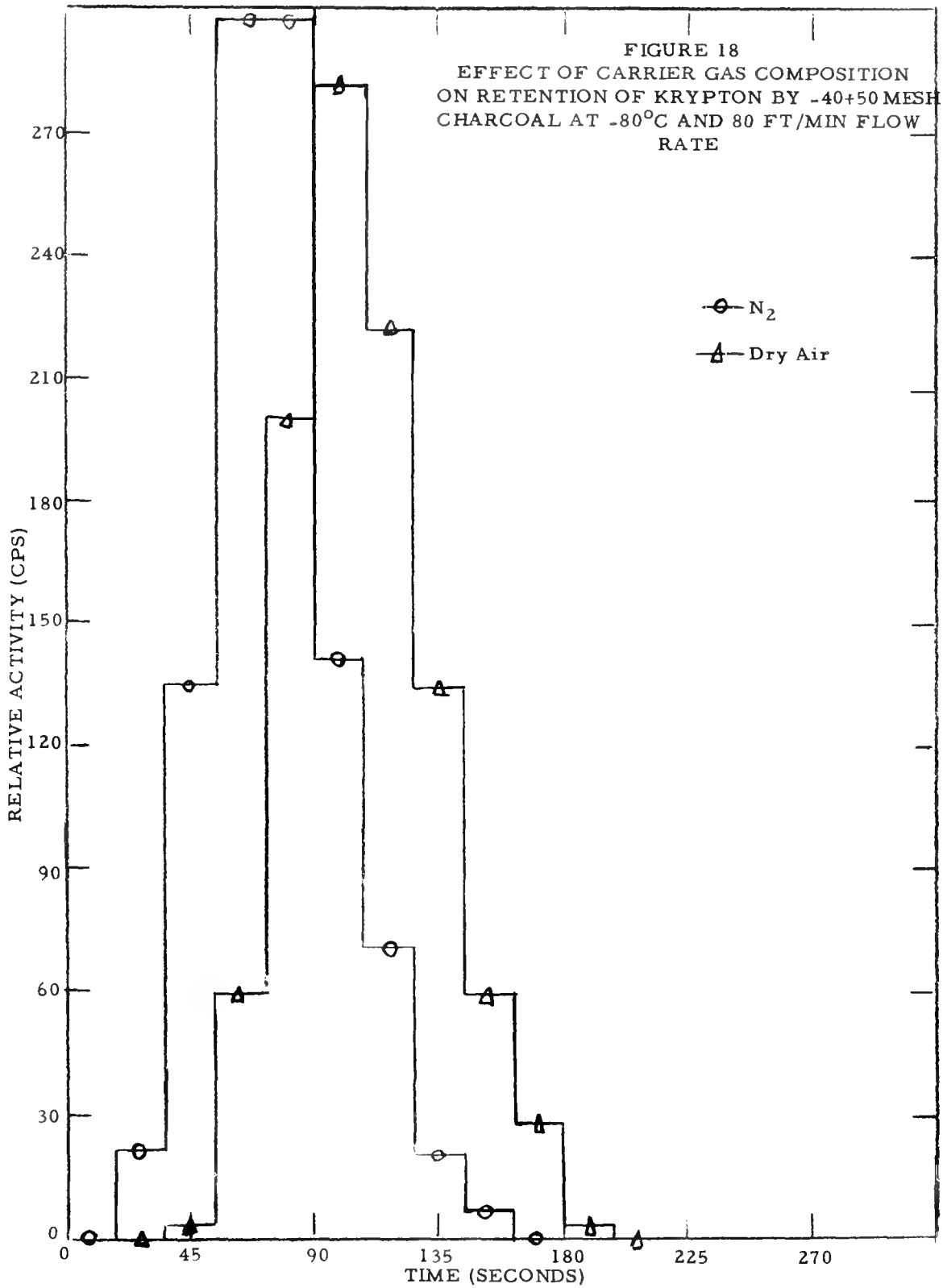

FIGURE 19
EFFECT OF CARRIER GAS COMPOSITION ON RETENTION OF KRYPTON BY -20+30 MESH CHARCOAL AT -80°C AND 40FT/MIN FLOW RATE

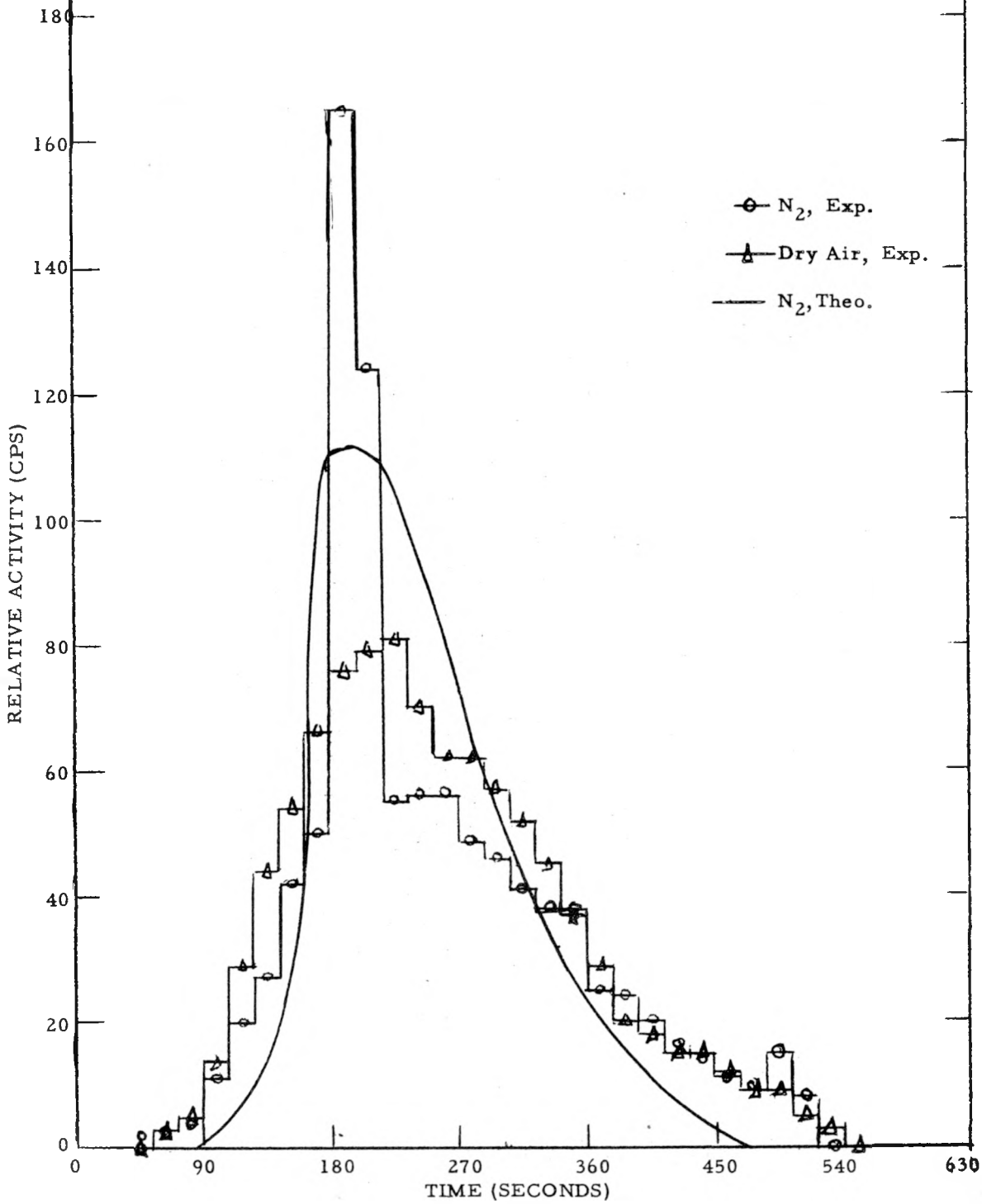

FIGURE 20
EFFECT OF CARRIER GAS COMPOSITION ON RETENTION OF KRYPTON BY -20+30 MESH CHARCOAL AT -80°C AND 80 FT/MIN FLOW RATE

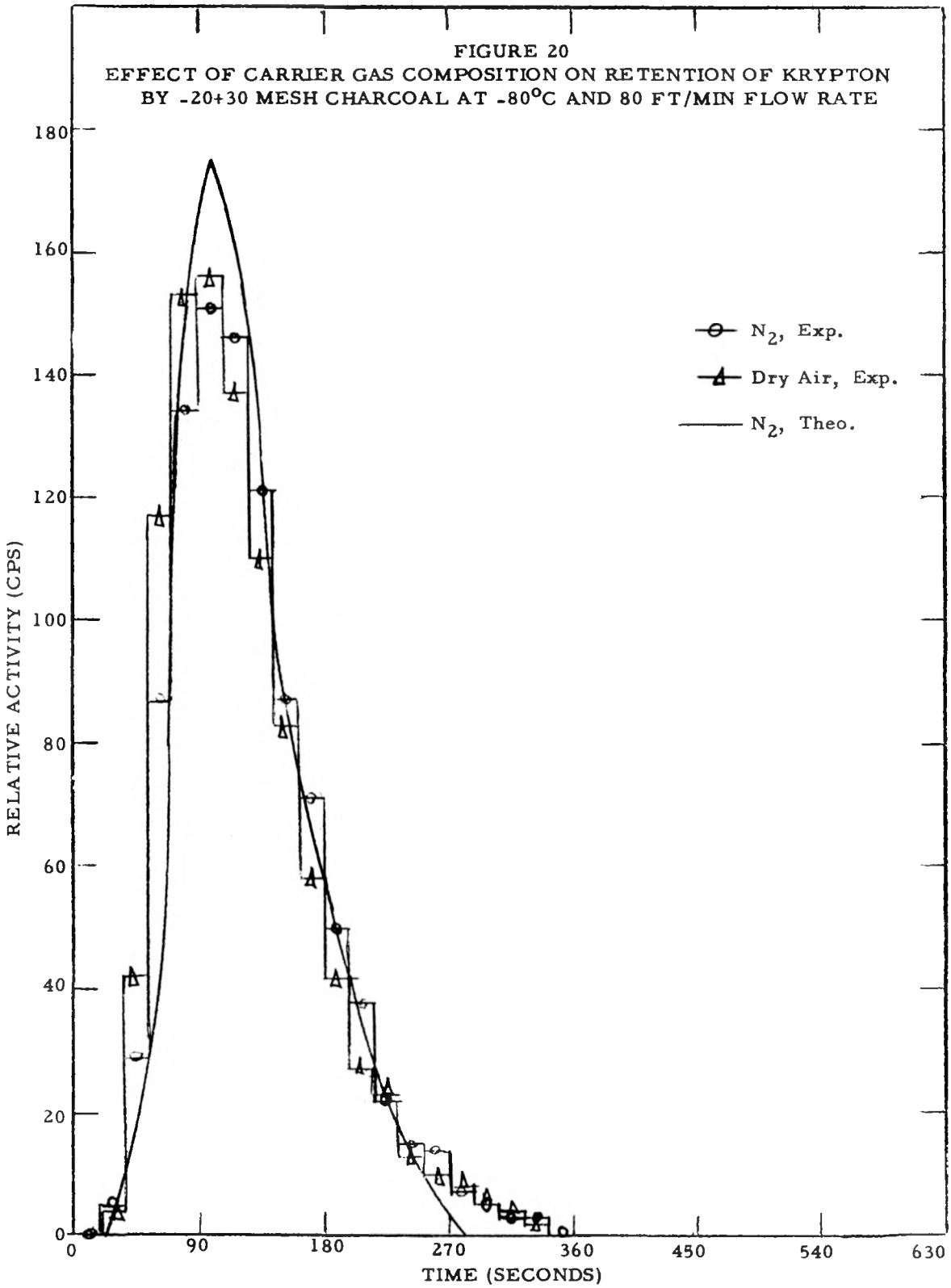

FIGURE 21
COMPARISON OF EXPERIMENTAL AND THEORETICAL
RETENTION EFFICIENCY FOR KRYPTON: -20+30 MESH
AT -80°C

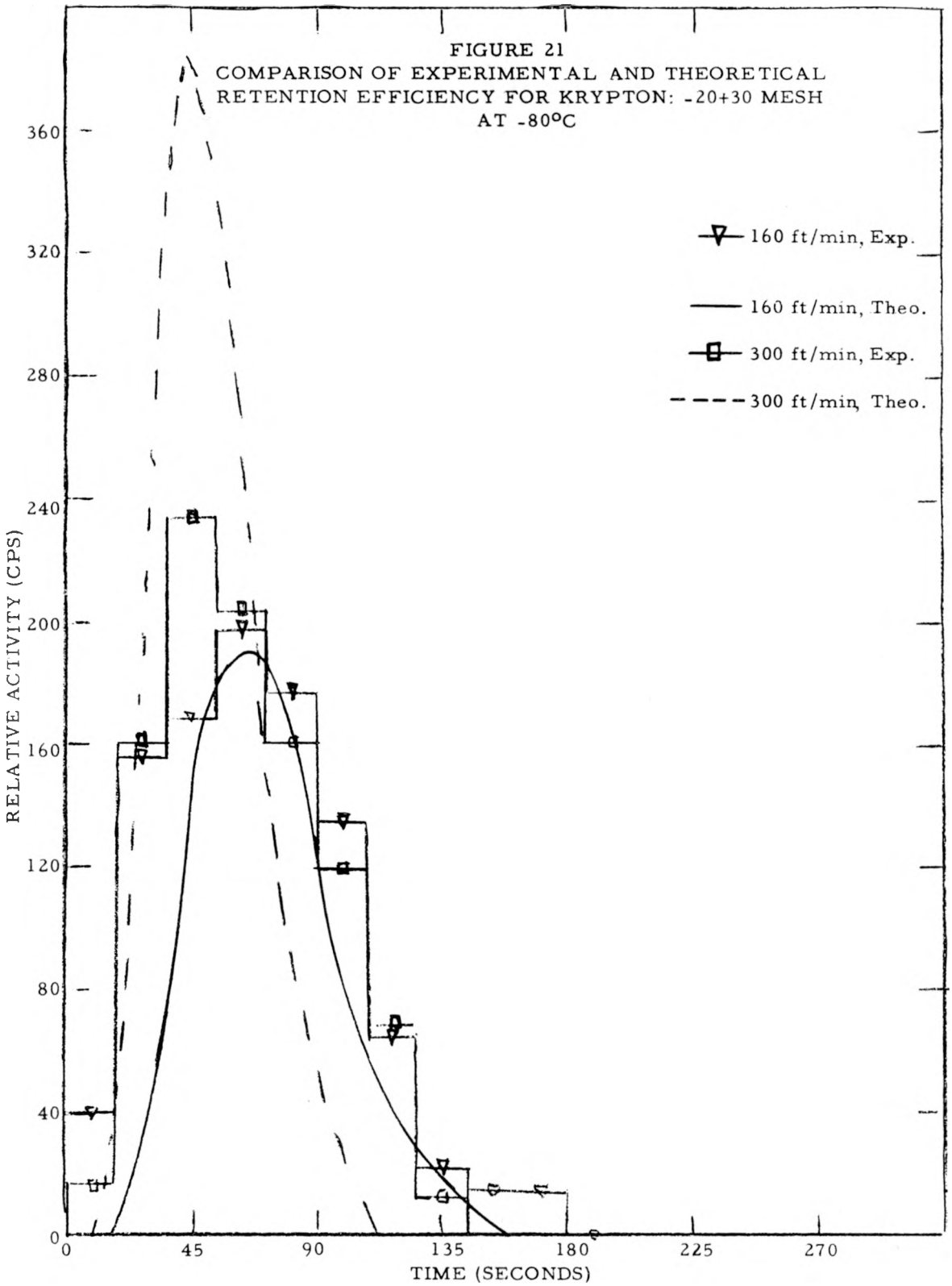

FIGURE 22
EFFECT OF FLOW RATE ON RETENTION OF XENON BY
-40+50 MESH CHARCOAL AT 100°C

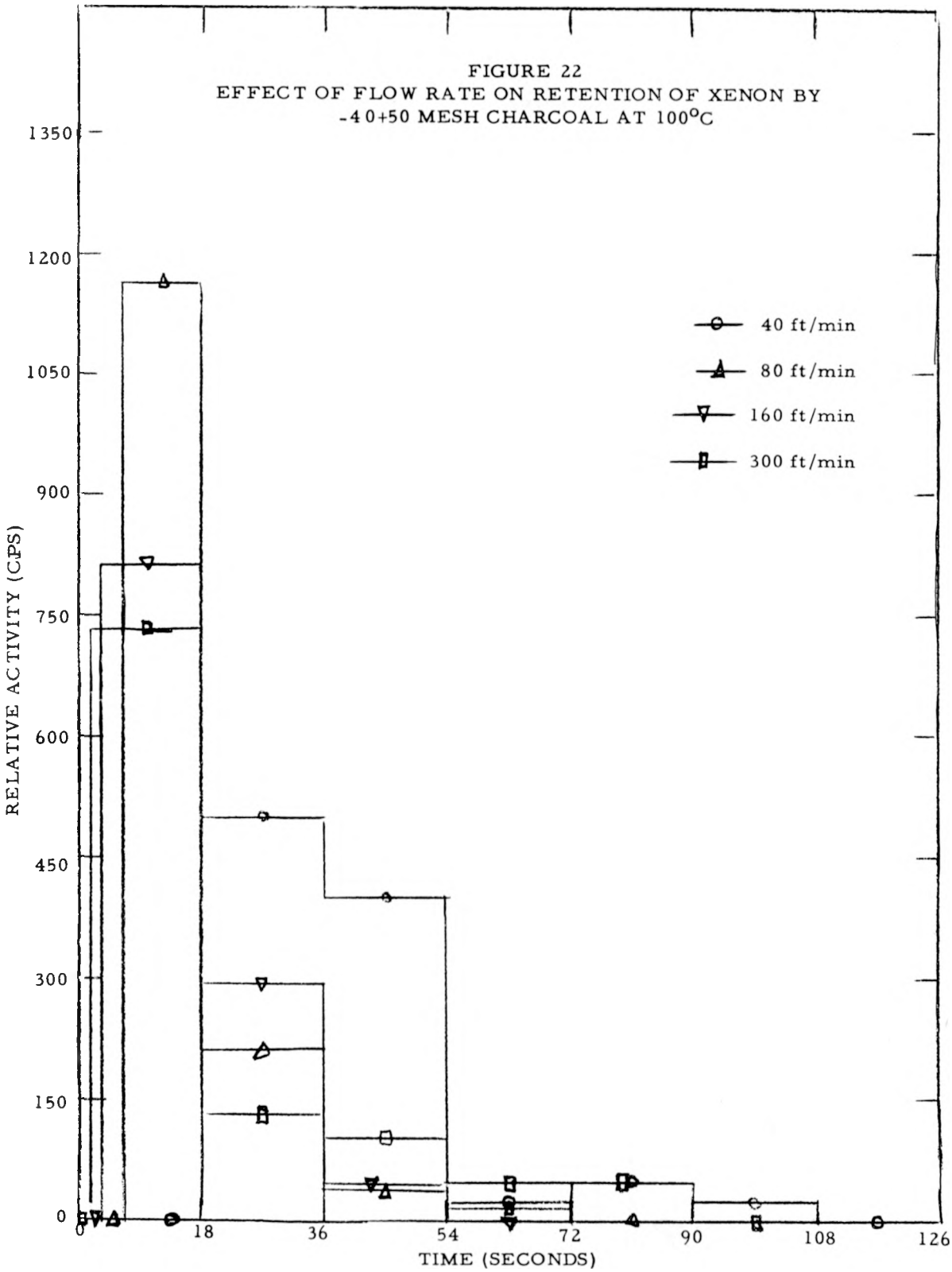

FIGURE 23
EFFECT OF FLOW RATE ON RETENTION OF XENON BY
-40+50 MESH CHARCOAL AT 0°C

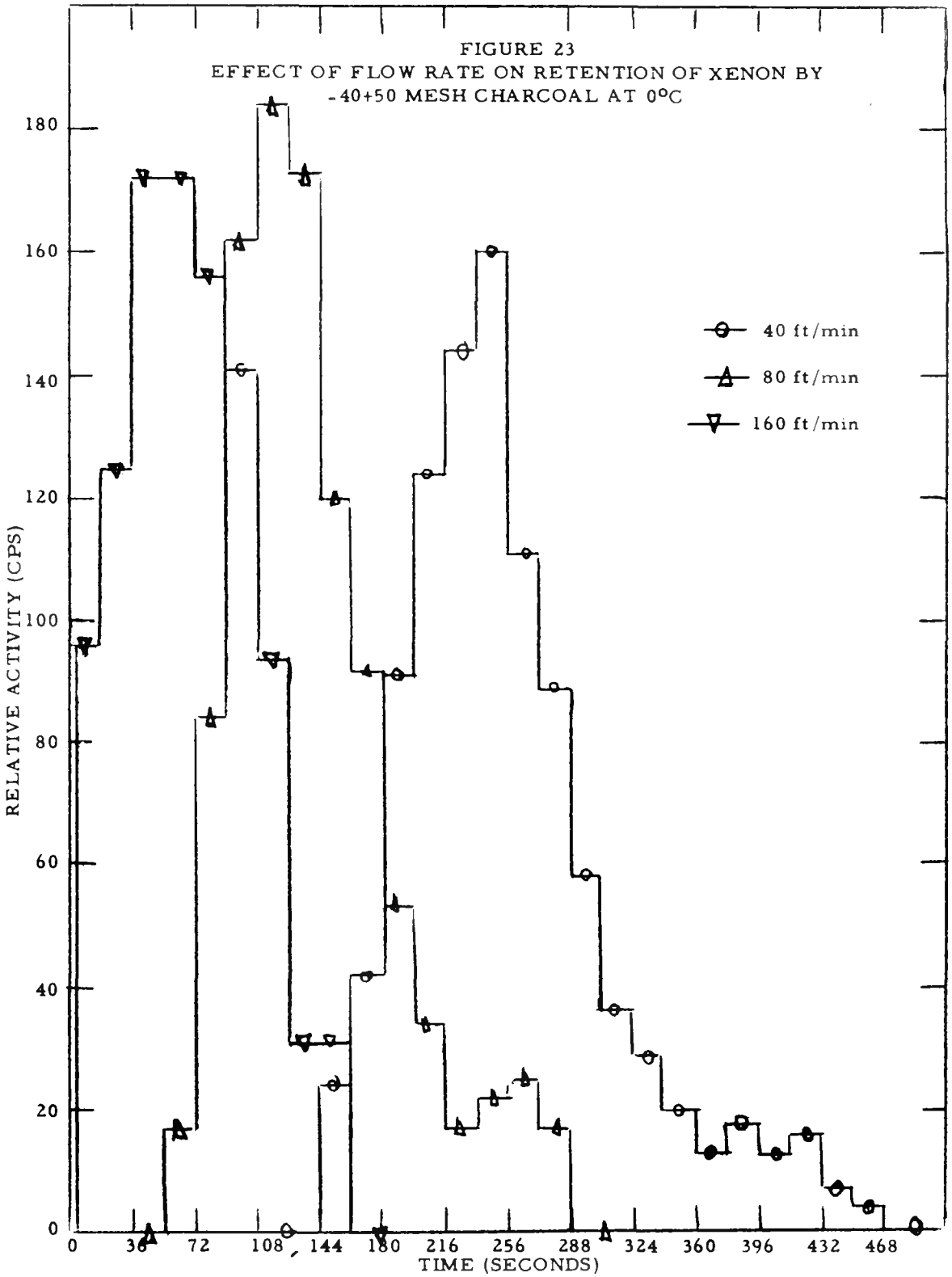

FIGURE 24
EFFECT OF TEMPERATURE ON RETENTION OF XENON BY
-40+50 MESH CHARCOAL AT 40FT/MIN FLOW RATE

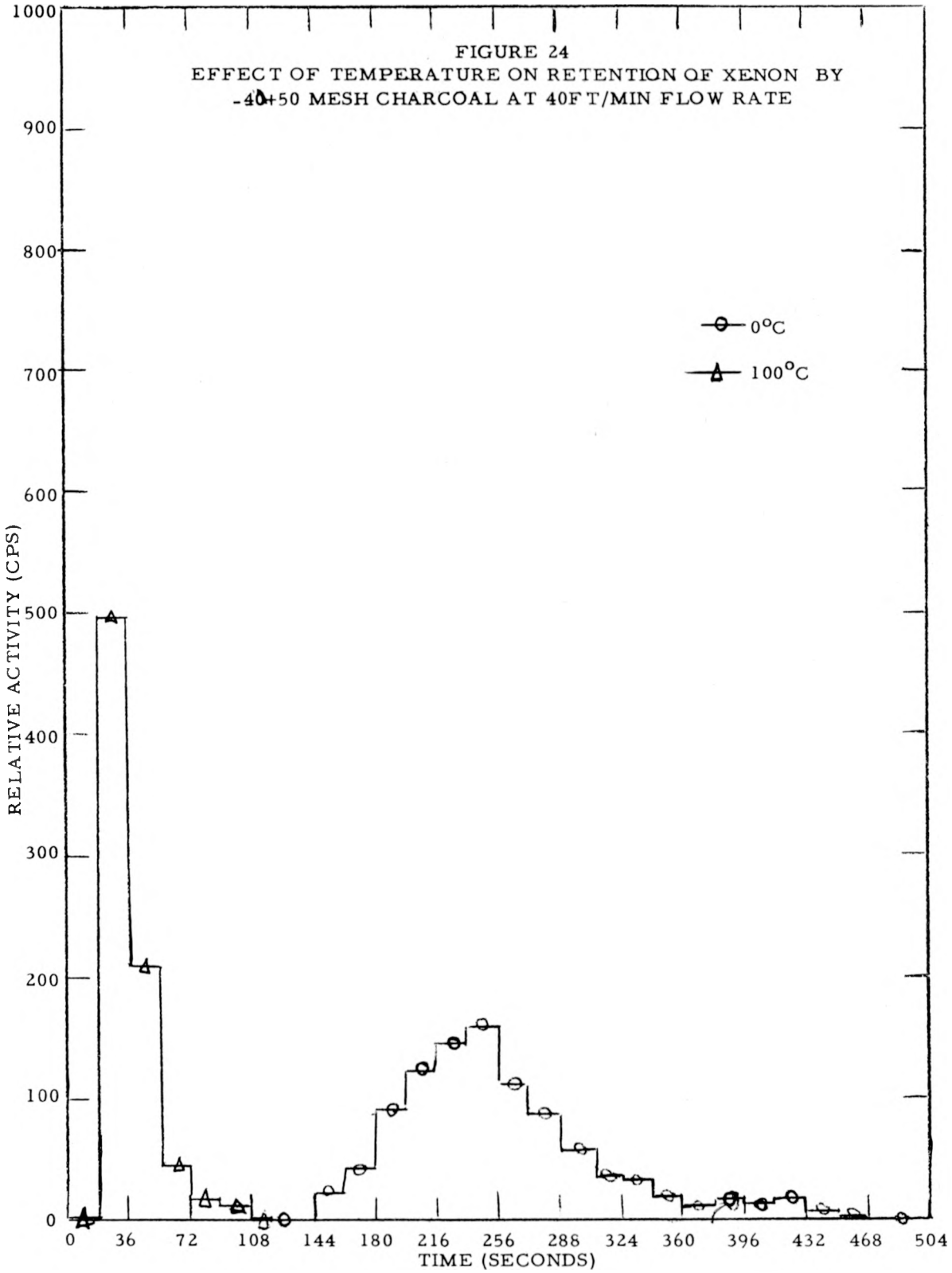

FIGURE 25
EFFECT OF TEMPERATURE ON RETENTION OF XENON BY
-40+50 MESH CHARCOAL AT 80 FT/MIN FLOW RATE

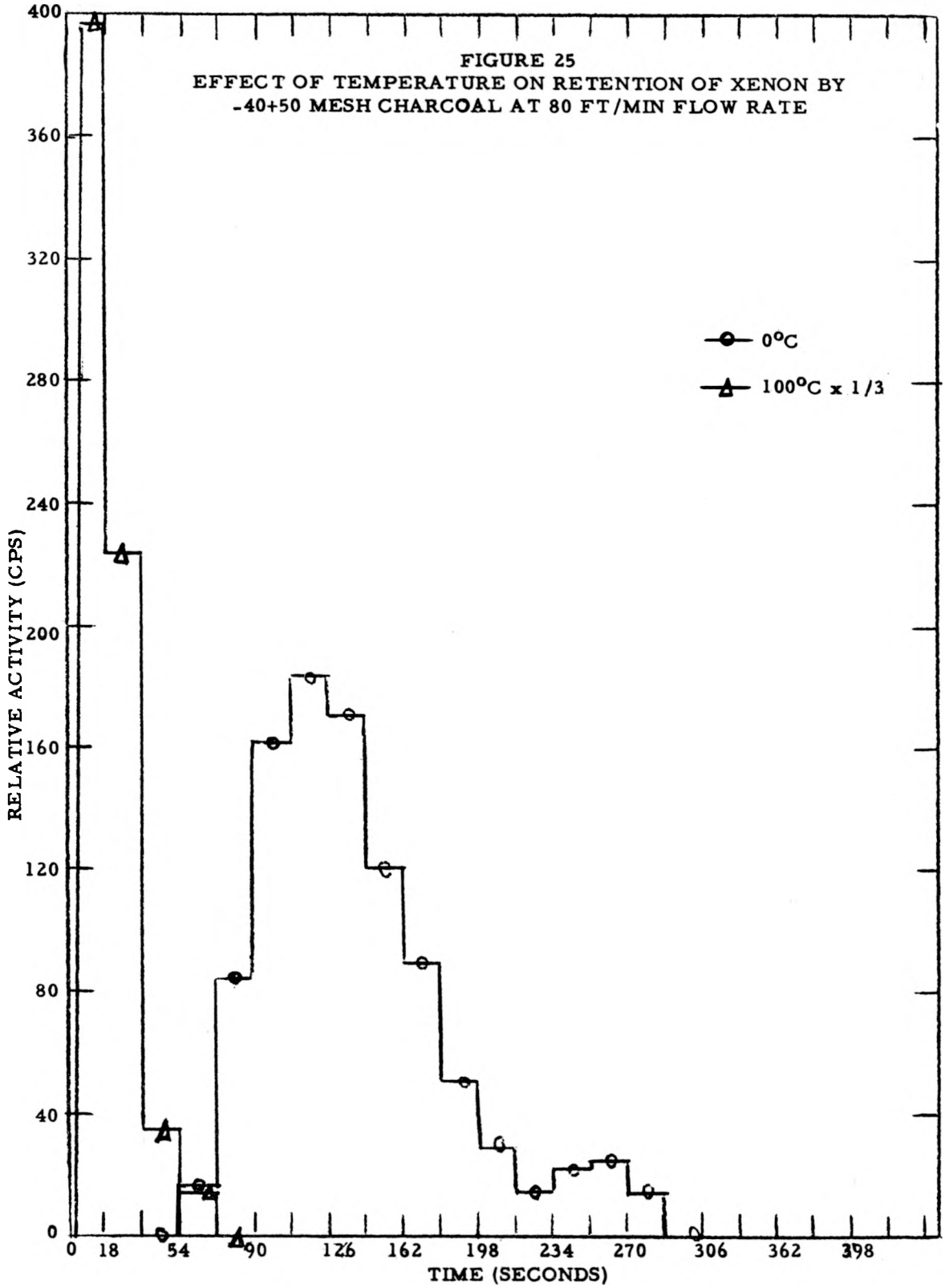

FIGURE 26
EFFECT OF TEMPERATURE ON RETENTION OF XENON BY
-40+50 MESH CHARCOAL AT 160 FT/MIN FLOW RATE

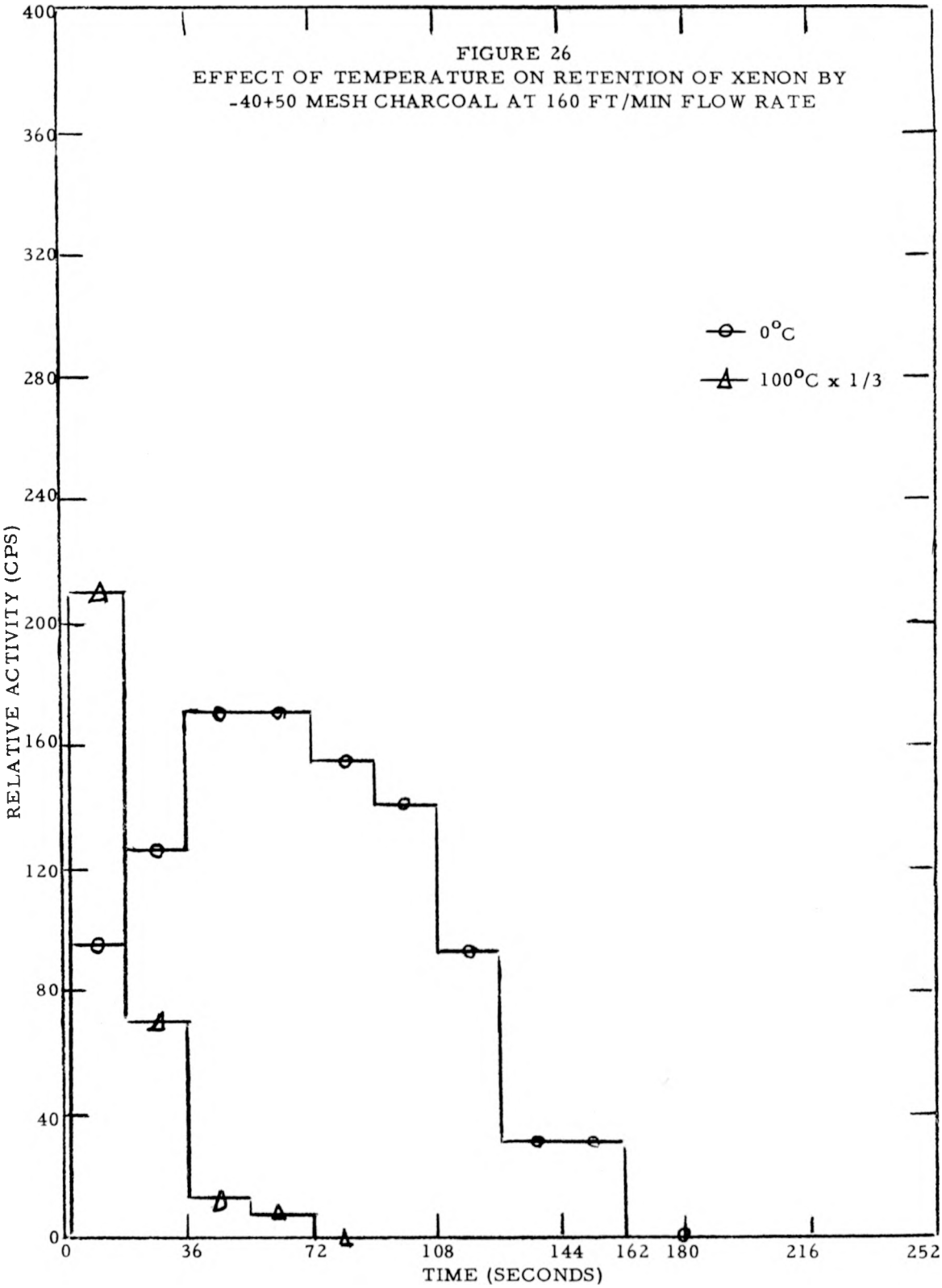

FIGURE 47
EFFECT OF FLOW RATE ON RETENTION OF XENON
BY -20+30 MESH CHARCOAL AT 100°C

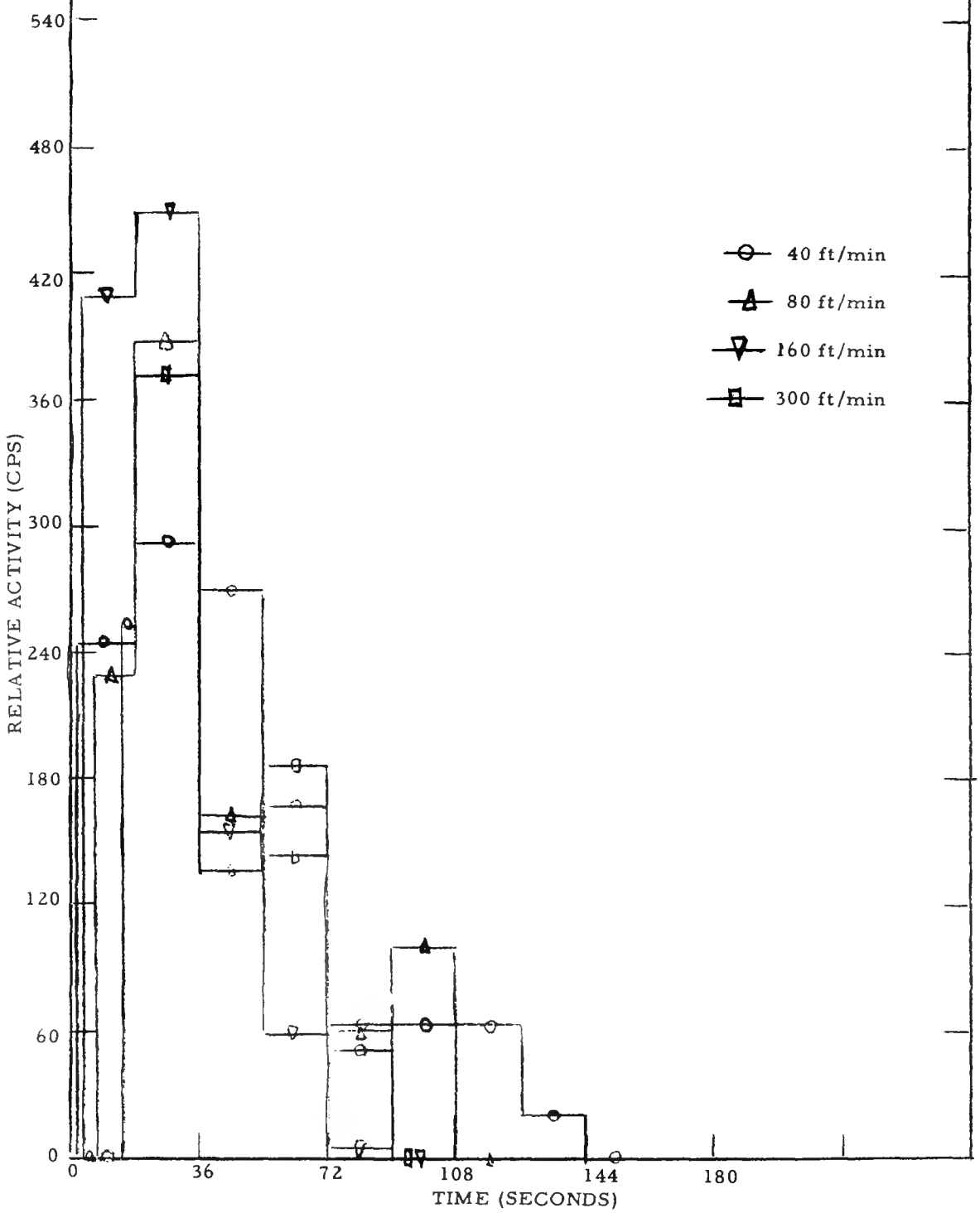

FIGURE 28
RETENTION OF XENON BY -20+30 MESH CHARCOAL AT 0°C

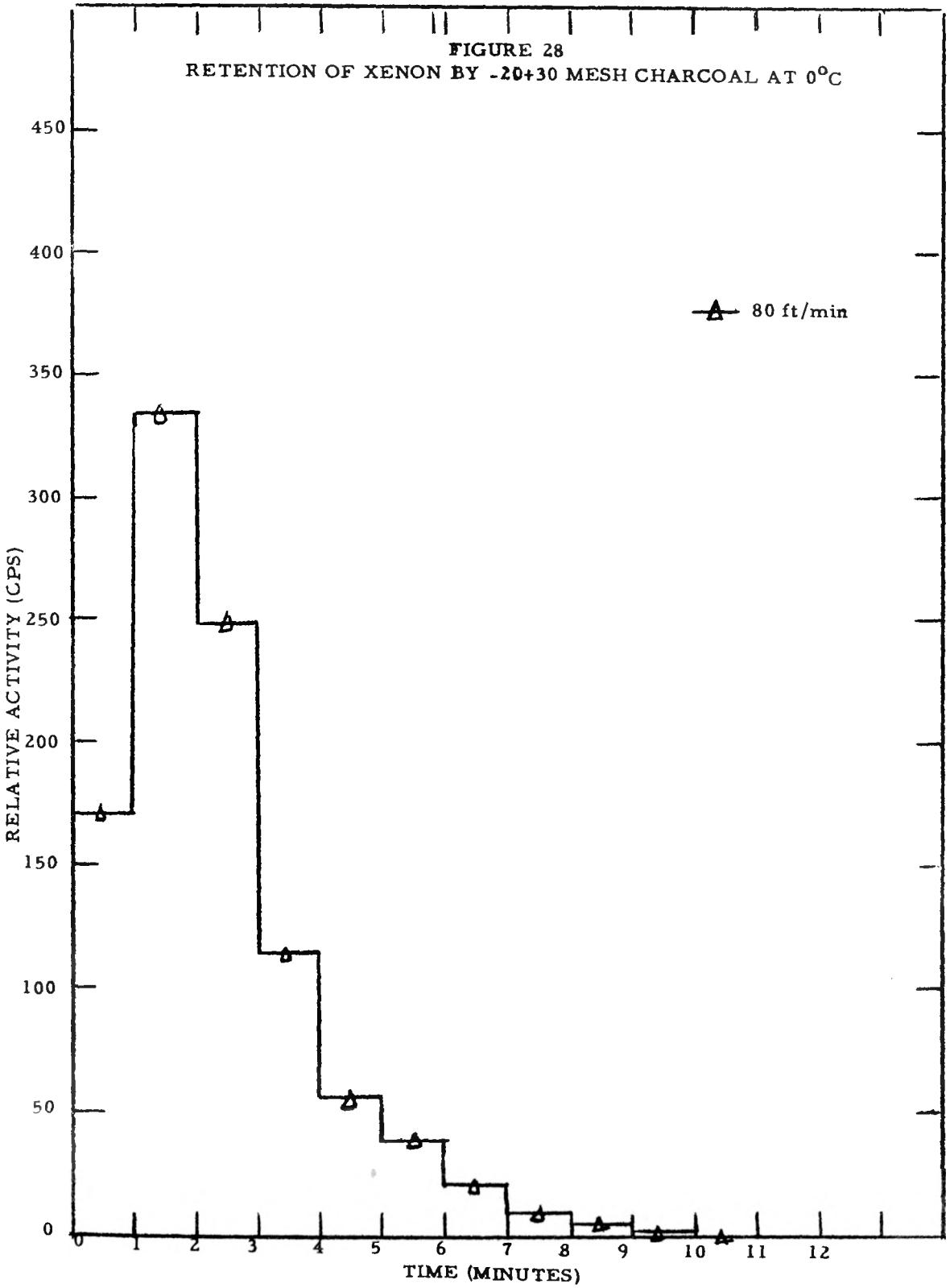

FIGURE 29
EFFECT OF FLOW RATE ON RETENTION OF XENON BY
-6+14 MESH CHARCOAL AT 100°C

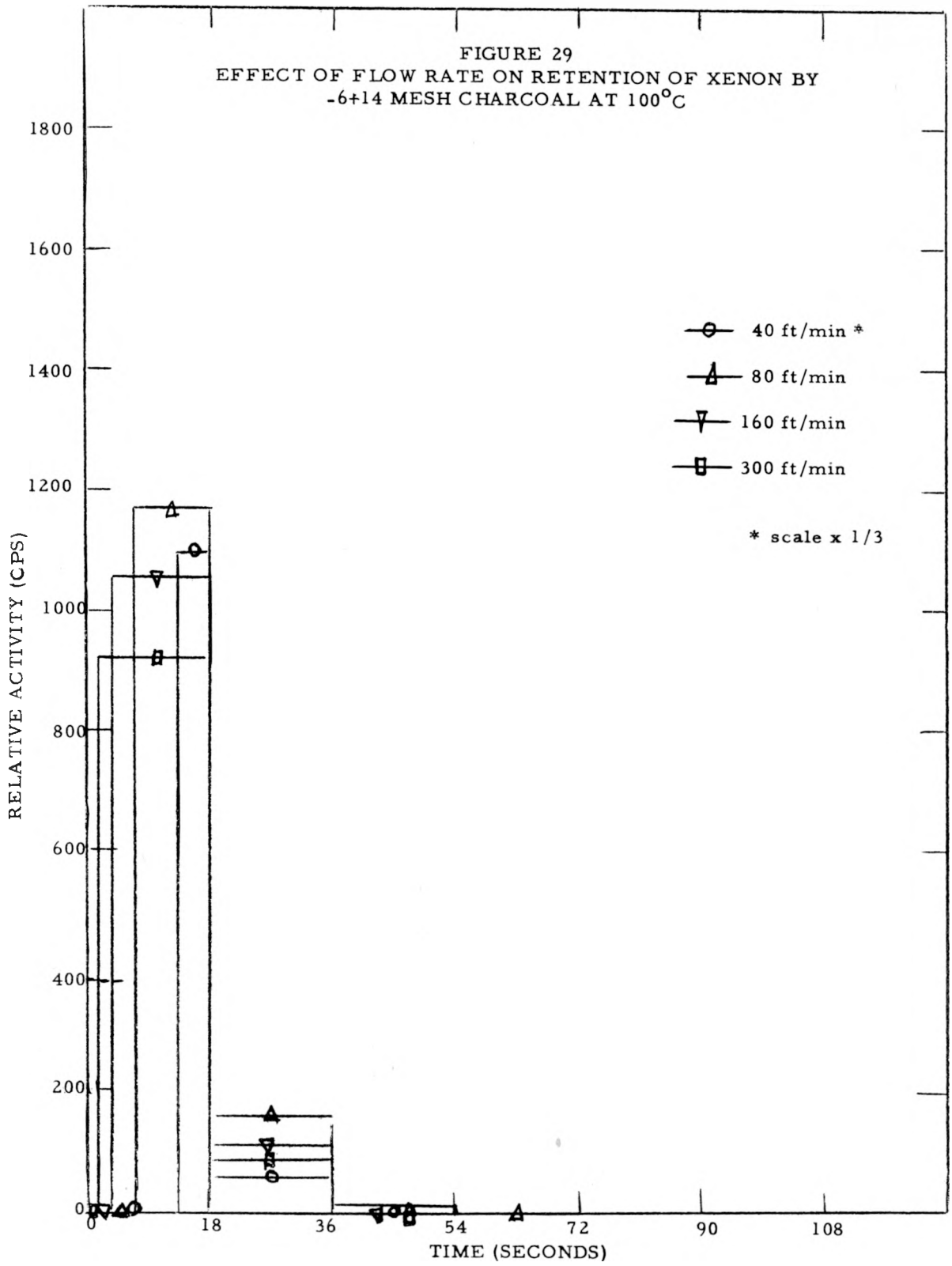

FIGURE 30
EFFECT OF FLOW RATE ON RETENTION OF XENON BY
-6+14 MESH CHARCOAL AT 0°C

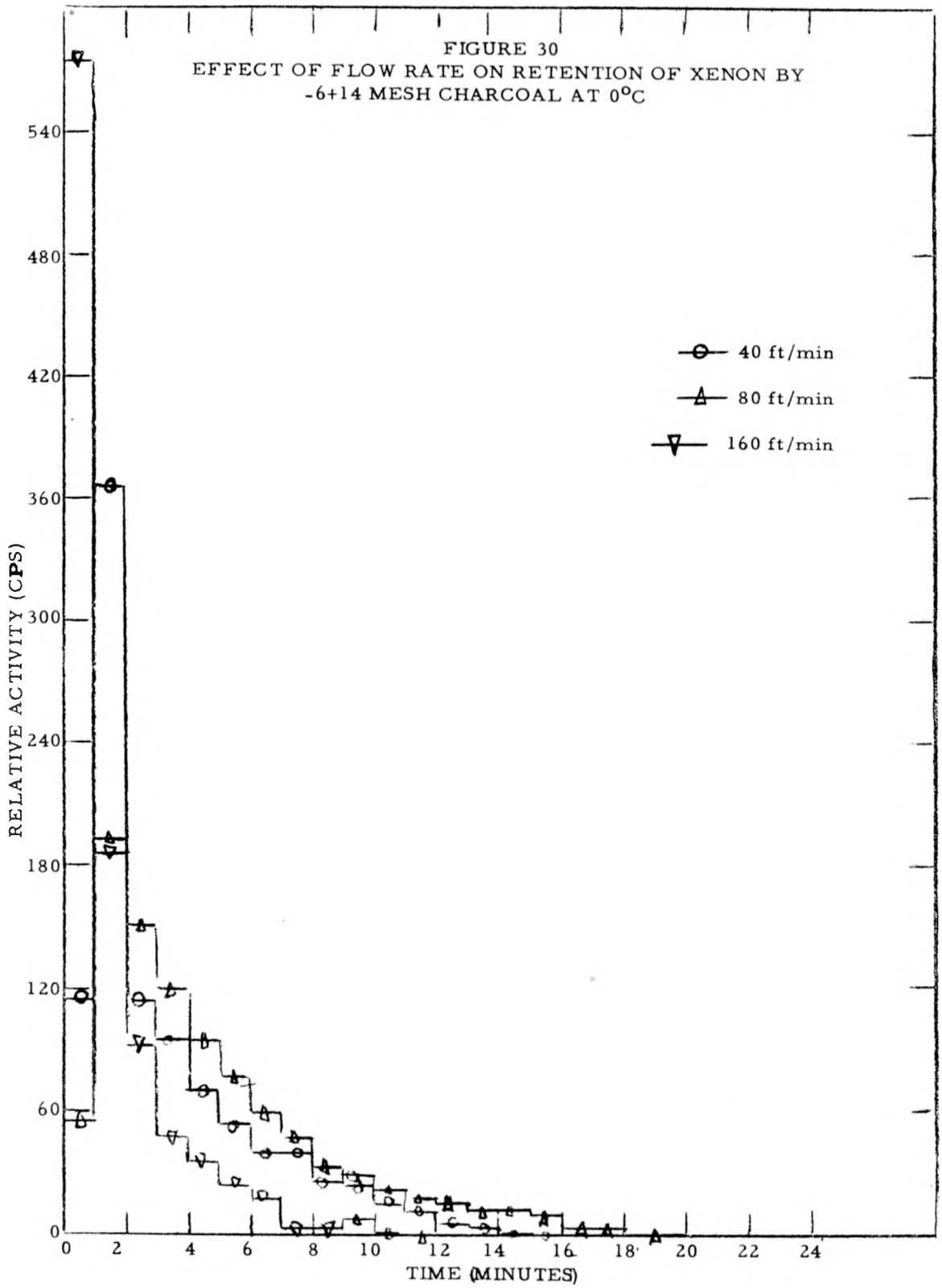

FIGURE 31
RETENTION OF XENON BY
-6+14 MESH CHARCOAL AT -80°C

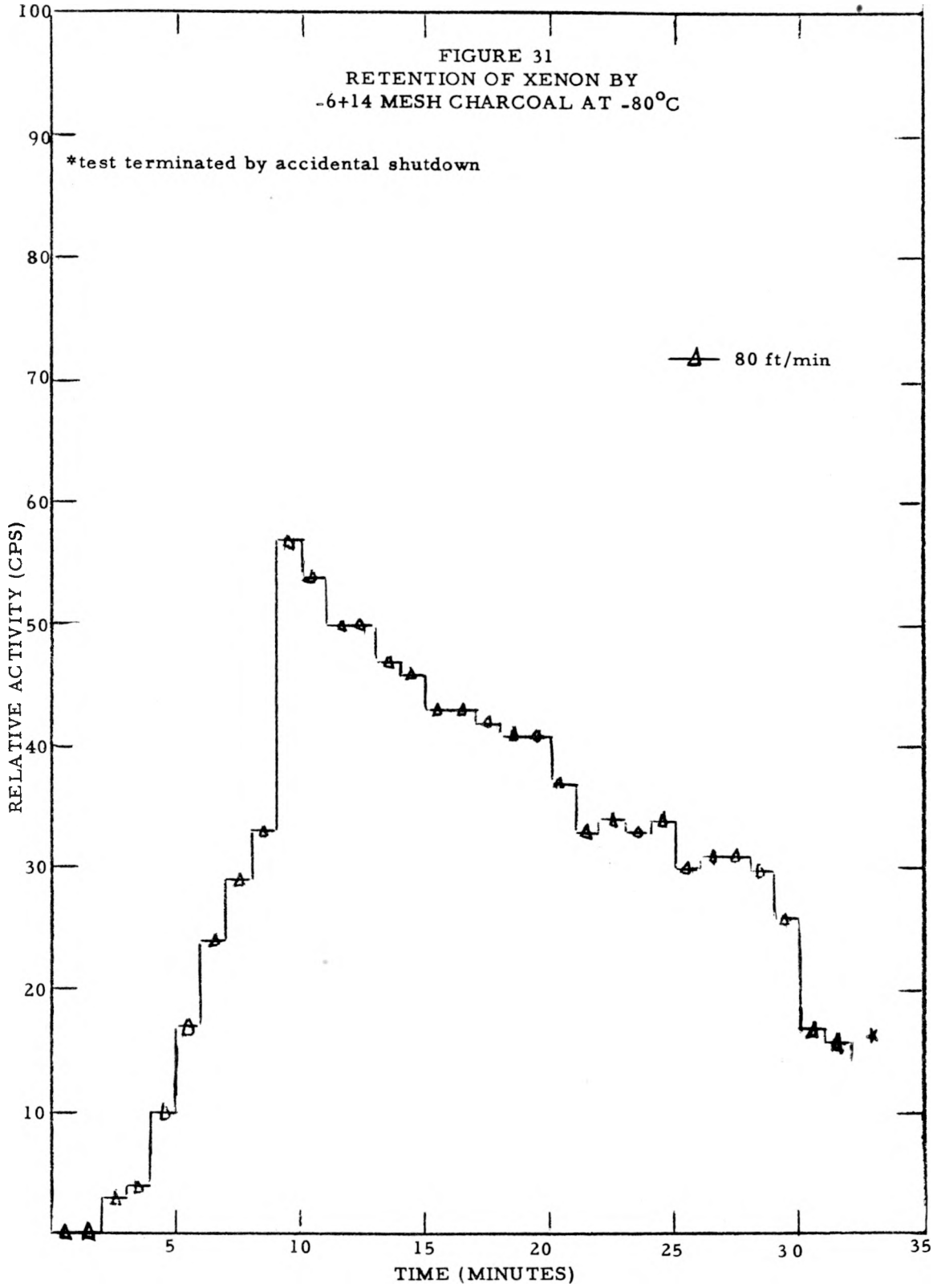

FIGURE 32
ADSORPTION CAPACITY OF -40+50 MESH CHARCOAL FOR KRYPTON

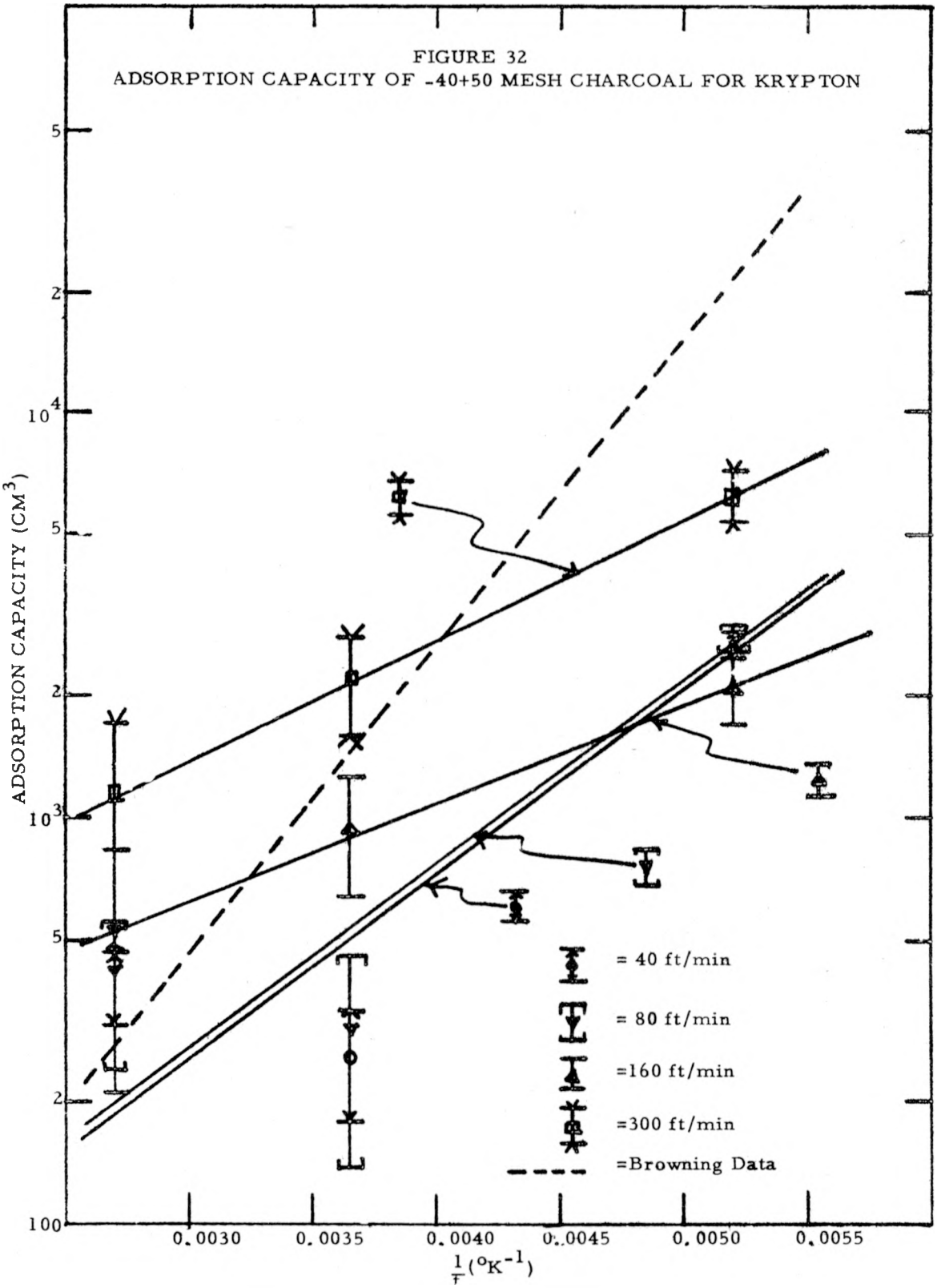

FIGURE 33
ADSORPTION CAPACITY OF -20+30 MESH CHARCOAL FOR KRYPTON

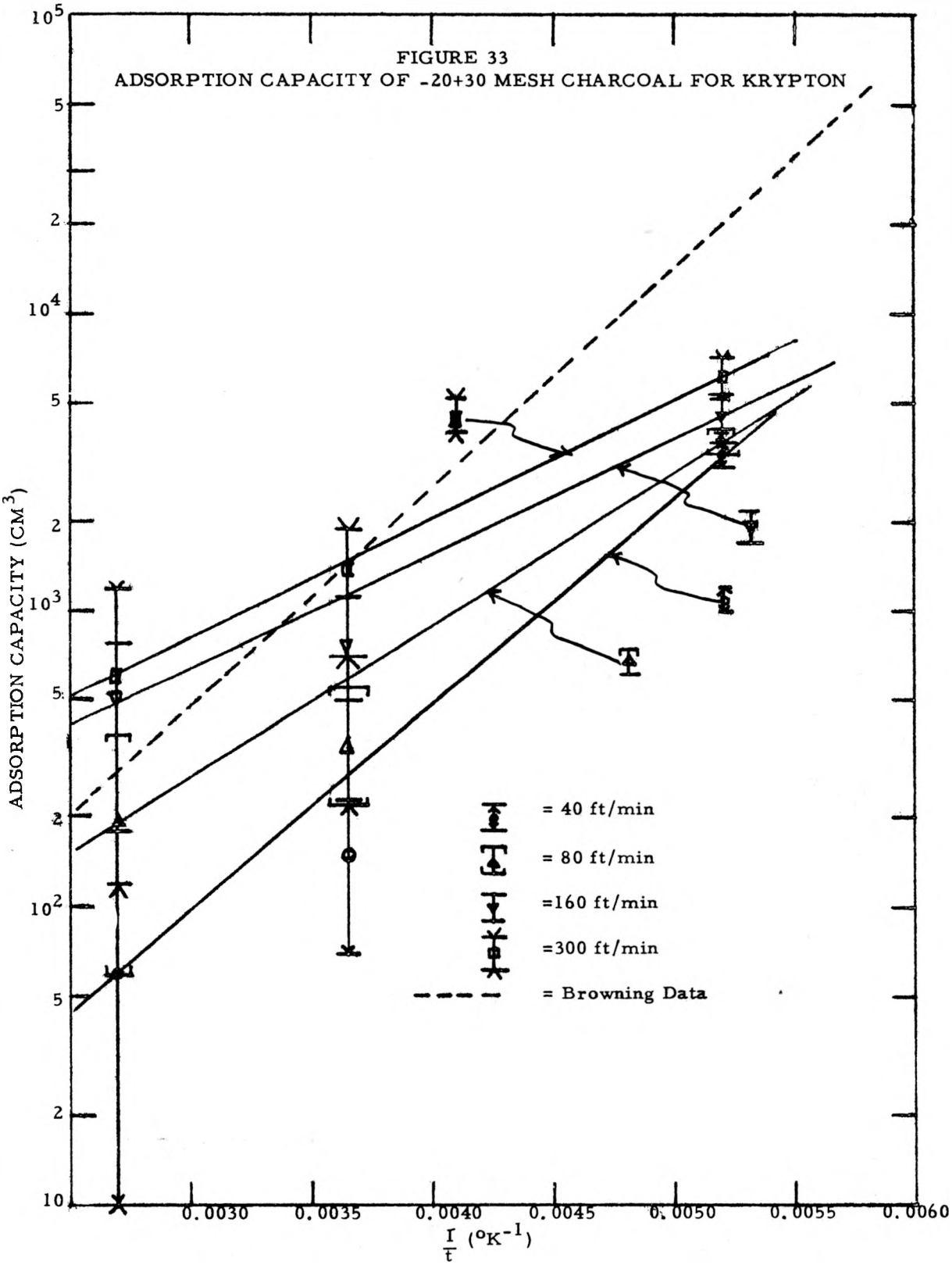

FIGURE 34
ADSORPTION CAPACITY OF -6+14 MESH CHARCOAL FOR XENON